2

Integrated modeling of vadose-zone flow and transport processes

M.T. van Genuchten[#] and Jirka Šimůnek[##]

Abstract

Enormous advances have been made during the past several decades in our understanding and ability to model flow and transport processes in the vadose zone between the soil surface and the groundwater table. A large number of conceptual models are now available to make detailed simulations of transient variably-saturated water flow, heat movement and solute transport in the subsurface. In this paper we highlight four examples illustrating such advances: (1) coupling physical and chemical processes, (2) simulating colloid and colloid-facilitated transport, (3) integrated modeling of surface and subsurface flow processes, and (4) modeling of preferential flow in the subsurface. The examples show that improved understanding of underlying processes, continued advances in numerical methods, and the introduction of increasingly powerful computers now permit us to make comprehensive simulations of the most important coupled, non-linear physical, chemical and biological processes operative in the unsaturated zone.

Introduction

Agricultural practices for supplying food to locally burgeoning populations were probably first implemented some 10,000 years ago in Eurasia, Africa and the Americas (Lawton and Wilke 1979). Hunting activities and gathering food were slowly complemented, or even replaced, by efforts to cultivate the Earth. This involved modifying the landscape to grow agricultural crops, raising domesticated animals and, increasingly between roughly 8,000 and 3,000 years ago, practicing irrigation. Many parts of the world still show impressive remnants of ancient irrigation systems, such as chains-of-wells systems in China, the Middle and Near East, and North Africa. These systems from around 2500 years ago and onward, supplied water for domestic consumption and irrigation through sophisticated subsurface irrigation tunnels, also known as qanatz, kanats or karez (e.g. Cressey 1958; Lawton and Wilke 1979). Some of these chains-of-wells systems are still in use today in the Middle East, China and elsewhere.

The ancient irrigation structures and related soil-management and irrigation practices, were at the time implemented without the advantage of modern computational tools, such as computers and sophisticated numerical methods, and hence without

---

[#] George E. Brown, Jr. Salinity Laboratory, USDA, ARS, 450 West Big Springs Road, Riverside, CA, 92557, USA. E-mail: rvang@ussl.ars.usda.gov

[##] Department of Environmental Sciences, University of California, Riverside, CA, 92521, USA. E-mail: jiri.simunek@ucr.edu

detailed conceptual-numerical descriptions based on equations governing water flow and chemical transport into and through the unsaturated zone. Against the long human history of manipulating soils and water for improved agricultural practices, it is therefore amazing that Darcy's law for saturated flow was first proposed only some 150 years ago (Darcy 1856), while the Richards equation for unsaturated flow was first formulated barely 70 years ago (Richards 1931). This shows that, compared to the time periods of human history and the implementation of agricultural practices and irrigation, truly astonishing advancements have been made during the past 30 years or so in process-based descriptions of subsurface flow and transport processes, numerical analysis and computer hardware. We have come to a point in history where truly unique opportunities exist for developing models that integrate the most pertinent processes affecting water, heat and solute movement in the subsurface. Much of the research in subsurface flow and transport has historically progressed along mostly disciplinary lines (e.g., soil physics, hydrogeology, geochemistry, microbiology, plant physiology). As such, physical, chemical and microbiological processes were often studied and implemented in relative isolation. The same is true for studies of surface and subsurface flow processes, and for flow and transport in the vadose zone and in groundwater. The introduction of increasingly powerful computers, advanced numerical methods and improved understanding of subsurface flow and transport processes, now provide tremendous opportunities for integrating the various processes involved.

In this paper we highlight several exciting approaches for coupling physical, chemical and other processes into integrated descriptions of the subsurface, while focusing especially on the vadose zone. We will address (1) relatively standard approaches for modeling flow and transport, (2) multicomponent geochemical transport, (3) colloid and colloid-facilitated transport, (4) integrated surface/subsurface modeling, and (5) process-based descriptions of preferential flow. We start with a relatively standard description of water, heat and solute movement.

Standard descriptions for water, heat and solute movement

Predictions of water, heat and solute movement in the vadose zone are traditionally made using the Richards equation for variably-saturated water flow and advection–dispersion type equations for heat and solute movement. For a one-dimensional soil profile these equations are given by e.g., Šimůnek, Šejna and Van Genuchten (1998)

$$\frac{\partial \theta}{\partial t} = \frac{\partial}{\partial z}[K(h)\frac{\partial h}{\partial z} - K(h)] - S \tag{1}$$

$$\frac{\partial C_p(\theta)T}{\partial t} = \frac{\partial}{\partial z}[\lambda(\theta)\frac{\partial T}{\partial z}] - C_w\frac{\partial qT}{\partial z} - C_w ST \tag{2}$$

$$\frac{\partial(\rho s)}{\partial t} + \frac{\partial(\theta c)}{\partial t} = \frac{\partial}{\partial z}(\theta D \frac{\partial c}{\partial z} - qc) - \phi \tag{3}$$

respectively, where θ is the volumetric water content (-), h is the soil water pressure head (L), t is time (T), z is distance from the soil surface downward (L), K is the hydraulic conductivity (LT^{-1}) as a function of h or θ, λ is the apparent thermal conductivity of the soil (MLT^{-3}K^{-1}), C_p and C_w are volumetric heat capacities (ML^{-1}T^{-2}K^{-1}) of the porous

medium and the liquid phase, respectively; T is temperature (K), s is the solute concentration associated with the solid phase of the soil (MM^{-1}), c is the solute concentration of the liquid phase (ML^{-3}), ρ is the soil bulk density (ML^{-3}), D is the solute dispersion coefficient (L^{2}T^{-1}), q is the volumetric fluid flux density (LT^{-1}) given by Darcy's law, and S (T^{-1}) and ϕ (M L^{-3} T^{-1}) are sinks or sources for water and solutes, respectively.

Equations (1) through (3) are relatively standard in that they have been popularly used for the past 50 years or so in various forms, simplifications or extensions. Examples of possible extensions are their use in two or three dimensions (Šimůnek, Huang and Van Genuchten 1995; Zyvoloski et al. 1997; Pruess, Oldenburg and Moridis 1999), the inclusion of vapor-phase transport (Scanlon et al. 2003) and volatilization (e.g. Jury, Spencer and Farmer 1983), extensions to multiphase flow involving separate flow equations for each fluid involved, such as water, air and/or oil (e.g. Pinder and Abriola 1986; Pruess and Battistelli 2002), multicomponent geochemical transport (Yeh and Tripathi 1990; Lichtner 2000), and incorporation of dual-porosity or dual-permeability formulations for preferential flow in macroporous soils or fractured rock (e.g. Gerke and Van Genuchten 1993; Šimůnek et al. 2003; Bodvarsson, Ho and Robinson 2003). Several of these and related studies have resulted in detailed codes such as TOUGH2 (Pruess, Oldenburg and Moridis 1999), the HYDRUS codes (Šimůnek, Šejna and Van Genuchten 1998; 1999), FEHM (Zyvoloski et al. 1997), HYDROBIOGEOCHEM (Yeh et al. 1998), RZWQM (Ahuja et al. 1999) and SWAP (Van Dam et al. 1997), among many others.

Much of the work presented in this paper is based on the HYDRUS codes (Šimůnek, Šejna and Van Genuchten 1998; 1999), but further modified to enable simulations of the four types of problems considered here (i.e., multicomponent geochemical transport, colloid and colloid-facilitated transport, integrated surface/subsurface modeling, and preferential/non-equilibrium flow and transport). For this reason we first give a brief summary of these codes. The HYDRUS-1D and HYDRUS-2D software packages are finite-element numerical models for simulating the one- or two-dimensional movement of water, heat and multiple solutes in variably saturated media. The programs numerically solve the Richards equation for variably-saturated water flow and advection–dispersion equations for heat and solute transport.

The solute transport equations in HYDRUS consider advective–dispersive transport in the liquid phase, and diffusive transport in the gaseous phase. The transport equations also include provisions for non-linear and/or non-equilibrium reactions between the solid and liquid phases, linear equilibrium reactions between the liquid and gaseous phases, zero-order production and two first-order degradation reactions: one which is independent of other solutes, and one which provides the coupling between solutes involved in sequential first-order decay reactions. Figure 1 shows a schematic of the sequential first-order decay chain reactions incorporated in the HYDRUS codes. Typical examples of sequential first-order decay chains are radionuclides (e.g. Lester, Jansen and Burkholder 1975; Rogers 1978; Van Genuchten 1985), nitrification/denitrification chains (e.g. Misra, Nielsen and Biggar 1974; Wagenet and Hutson 1987; Ahuja et al. 1999), organic-phosphate transport (Castro and Rolston 1977), pesticide decay chains (e.g. Bromilow and Leistra 1980; Wagenet and Hutson 1987), chlorinated-hydrocarbon decay chains (PCE to TCE to ethylene) (Schaerlaekens et al. 1999; Casey and Šimůnek 2001), pharmaceuticals (Casey et al. 2003; 2004), explosives and energetics (Selim, Xue and Iskandar 1995; Sheremata et al. 1999) and other contaminants.
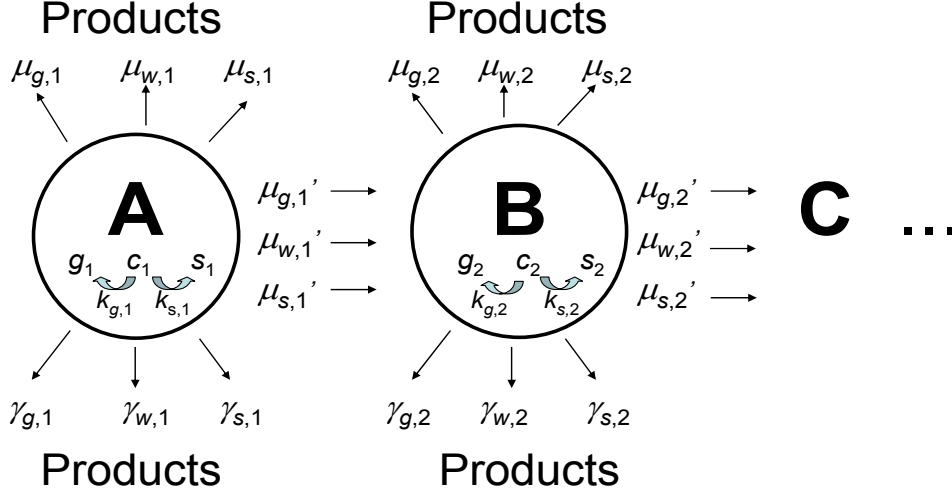
Figure 1. Schematic of system of solutes subject to zero-order production/decay and sequential first-order degradation chain reactions, where c (ML^{-3}), s (MM^{-1}), and g (ML^{-3}) represent concentrations in the liquid, solid and gaseous phases, respectively; the subscripts s, w, and g refer to solid, liquid and gaseous phases, respectively; straight arrows represent the different zero-order (γ) and first-order (μ, μ') rate reactions, and k_g and k_d indicate equilibrium distribution coefficients between phases

Incorporation of the decay chain reactions of Figure 1 into Eq. (3) leads to the following set of transport equations (Šimůnek, Šejna and Van Genuchten 1998):

$$\frac{\partial \theta c_k}{\partial t} + \frac{\partial \rho s_k}{\partial t} + \frac{\partial a_v g_k}{\partial t} = \frac{\partial}{\partial z}\left(\theta D_k^w \frac{\partial c_k}{\partial z}\right) + \frac{\partial}{\partial z}\left(a_v D_k^g \frac{\partial g_k}{\partial z}\right) - \frac{\partial q c_k}{\partial z} -$$

$$- (\mu_{w,k} + \mu'_{w,k})\theta c_k - (\mu_{s,k} + \mu'_{s,k})\rho s_k - (\mu_{g,k} + \mu'_{g,k})a_v g_k + \mu'_{w,k-1}\theta c_{k-1} +$$

$$+ \mu'_{s,k-1}\rho s_{k-1} + \mu'_{g,k-1}a_v g_{k-1} + \gamma_{w,k}\theta + \gamma_{s,k}\rho + \gamma_{g,k}a_v - S\,c_{r,k} \quad k = 2,3,...,n_s \tag{4}$$

where μ_w, μ_s, and μ_g are first-order rate constants (T^{-1}) for solutes in the liquid, solid and gas phases, respectively; μ_w', μ_s', and μ_g' are similar first-order rate constants (T^{-1}) providing connections between individual chain species, γ_w, γ_s, and γ_g are zero-order rate constants for the liquid (ML^{-3}T^{-1}), solid (T^{-1}), and gas (ML^{-3}T^{-1}) phases, respectively; a_v is the air content, S is the sink (T^{-1}) term in the water flow equation (1), c_r is the concentration of the sink term, D^w is the dispersion coefficient for the liquid phase (L^{2}T^{-1}), and D^g is the diffusion coefficient for the gas phase (L^{2}T^{-1}). As before, the subscripts w, s, and g correspond with the liquid, solid and gas phases, respectively; the subscript k represents the kth chain number, and n_s is the number of solutes involved in the chain reaction. While seemingly complicated because of the many terms involved, the basic concepts of Eq. (4) are relatively straightforward. Also, application of models based on the above equations is greatly facilitated by using graphical interfaces (GUI), such as those implemented in the HYDRUS software packages (www.hydrus2d.com).

Multicomponent geochemical transport

Equation (3) provides a highly simplified approximation for solute transport in many applications in that the model considers the transport of only a single species. Equation (4) is already more realistic by assuming that the solutes are subject to relatively simple consecutive decay chain reactions. Still, in general, both models ignore the fact that the soil liquid phase always contains a mixture of many ions that may interact, create complex species, precipitate, dissolve and/or compete with each other for sorption sites on the solid phase. The fate and transport of many naturally occurring elements and contaminants in the subsurface is affected by a multitude of complex, interactive physical, chemical, mineralogical and biological processes. For example, changes in the chemical composition or pH of the soil solution may impact the retention of heavy metals on organic matter or iron oxides. Dissolution and precipitation of minerals generally buffer the transport of a solution with a different pH through the soil profile. Simulation of these and related processes requires the use of a coupled multicomponent reactive transport code that integrates the physical processes of water flow and advective–dispersive solute transport with a range of possible biogeochemical processes. Below we give first a brief overview of multicomponent transport-modeling approaches, and then illustrate their use with two related examples, one for steady-state flow and one for variably-saturated conditions.

Overview of past and current research

Many important environmental problems require analysis of the coupled transport and reaction of multiple chemical species (Šimůnek and Valocchi 2002). Examples are acid mine drainage (Walter et al. 1994; Lichtner 1996), radionuclide transport (Viswanathan et al. 1998), the fate and transport of metal-organic mixed waste (Rittmann and VanBriesen 1996; VanBriesen 1998), analysis of redox zones in organic-contaminated aquifers (Abrams, Loague and Kent 1998; Essaid et al. 1995), and reactive permeable barriers for aquifer remediation (Fryar and Schwartz 1994). Multicomponent geochemical transport may need to be considered also in applications dealing with salinity management and evaluation of irrigation or drainage practices in arid and semiarid areas, including studies of the suitability of water for irrigation, drainage water reuse and the reclamation of sodic soils (e.g. Tanji 1990; Rhoades 1997; Šimůnek and Suarez 1997).

Multicomponent geochemical transport studies were initially limited mostly to the saturated zone where changes in the fluid velocity, temperature and pH are generally much more gradual and hence less important than in the unsaturated zone. Consequently, most multicomponent transport models assume one- or two-dimensional steady-state saturated water flow with fixed values for the flow velocity, water content (or porosity), temperature and/or pH (Valocchi, Street and Roberts 1981; Rubin 1983). Early examples for more general conditions involving major ion chemistry and cation exchange in unsaturated soils, generally using mixing cell approaches, are given by Dutt, Shaffer and Moore (1972), Robbins, Wagenet and Jurinak (1980), and Wagenet and Hutson (1987). Only recently have more generalized multicomponent transport models been developed which also consider variably-saturated flow. These include DYNAMIX (Liu and Narasimhan 1989), HYDROBIOGEOCHEM (Yeh and Tripathi 1990; Yeh et al. 1998), UNSATCHEM-2D (Šimůnek and Suarez 1994), FEHM (Zyvoloski et al. 1997), MULTIFLO (Lichtner and Seth 1996), and FLOTRAN (Lichtner 2000).

Geochemical transport models can be divided into several major groups, such as

models with specific chemistry, and more general, loosely coupled models often involving sequential iteration (Yeh and Tripathi 1990; Steefel and MacQuarrie 1996; Leij et al. 1999; Carrayrou, Mose and Behra 2004). Models with specific chemistry are generally limited in the number of species they can handle, while their application is usually restricted to problems having a prescribed chemical system. They are, however, much easier to use and computationally can be much more efficient than more general models. Typical examples of models with specific chemistry are those simulating the transport of major ions, such as UNSATCHEM (Šimůnek and Suarez 1994; 1997), or various reclamation models. Models with more generalized chemistry generally invoke a variety of sequential iterative or non-iterative operator-splitting approaches in which transport and chemistry are solved in separate steps (Steefel and MacQuarrie 1996; Bell and Binning 2004; Carrayrou, Mose and Behra 2004). Models of this type include the DYNAMIX, HYDROGEOCHEM, MULTIFLO, and FLOTRAN models mentioned earlier, as well as the OS3D/GIMRT code of Steefel and Yabusaki (1996). Such models provide users with far more freedom in designing their particular chemical system, and hence permit a much broader array of applications.

When the source terms and the decay and biodegradation reactions are neglected, multicomponent transport during one-dimensional transient variably-saturated flow may be described with the following set of equations (e.g. Šimůnek and Suarez 1994):

$$\frac{\partial \theta c_j}{\partial t} + \rho \frac{\partial (s_j + p_j)}{\partial t} = \frac{\partial}{\partial z}\left(\theta D \frac{\partial c_j}{\partial z}\right) - \frac{\partial q c_j}{\partial z} \qquad j = 1, 2, ..., n_s$$

(5)

where c_j (ML^{-3}), s_j (MM^{-1}) and p_j (MM^{-1}) are the total dissolved, sorbed/exchanged, and mineral (precipitated) concentrations, respectively, of aqueous component j, and n_s is the number of aqueous components. The second term on the left-hand side of (5) is absent for components that do not undergo ion exchange and precipitation/dissolution reactions. The total concentration of a component j, defined as the sum of the dissolved, sorbed and mineral concentrations, is influenced only by transport processes which act on the solution concentration c_j, but not by chemical reactions. However, the relative fraction of a component in each of the three phases (solution, sorbed, mineral) depends strongly on the specific chemical processes of the system being considered. Therefore, Eq. (5) must be augmented with equations describing the different equilibrium and non-equilibrium chemical reactions such as complexation, cation exchange, and precipitation/dissolution (Šimůnek and Valocchi 2002).

The more general geochemical transport-modeling approach was implemented in our recent work (Jacques et al. 2003) on multicomponent transport in which we coupled the HYDRUS-1D water flow and solute transport model (Šimůnek, Šejna and Van Genuchten 1998) with the PHREEQC geochemical speciation model (Parkhurst and Appelo 1999). PHREEQC considers a variety of chemical reactions such as aqueous speciation; gas, aqueous and mineral equilibrium; oxidation–reduction reactions; and solid-solution, surface-complexation, ion-exchange and kinetic reactions. The HYDRUS-1D and PHREEQC models were coupled using a non-iterative operator-splitting approach (SNIA), which first solves the water flow and solute transport part of the problem, and then the geochemical part. The combined HYDRUS1D-PHREEQC model (Jacques et al. 2003) permits simultaneous simulations of variably-saturated transient water flow, multicomponent solute transport, and speciation and other geochemical processes, including a broad range of mixed equilibrium and kinetic reactions.

The following two examples, taken from Jacques et al. (2003), illustrate the potential power and versatility of the loosely coupled multicomponent geochemical modeling approach used in HYDRUS1D-PHREEQC. The first example simulates heavy-metal transport in a multi-layered soil profile assuming steady-state water flow and pH-dependent cation exchange capacities. The second example extends the analysis to variably-saturated flow by simulating the long-term fate and transport of heavy metals under transient field conditions.

Example for steady-state flow

This example considers the transport of several major cations (Na, K, Ca, Mg) and three heavy metals (Cd, Zn, Pb) in a 50-cm deep multi-layered soil profile having different soil hydraulic properties and pH-dependent cation exchange capacities (CECs). Assuming that the CEC is associated solely with organic matter, the cation exchange capacity will increase significantly with increasing pH due to the acid-base properties of its functional groups. This behavior is represented by a multi-site cation exchange complex consisting of six sites, each having a different selectivity coefficient for the exchange of protons (Appelo, Verweij and Schafer 1998). The top 28 cm of the soil was assumed to be contaminated with the three heavy metals (initial pH 8.5), while an acid metal-free solution (pH 3) infiltrated into the soil. Flow was assumed to be steady-state at a relatively low constant flux density of 0.05 cm day^{-1}, which caused the soil profile to be unsaturated (water content values varied between 0.37 and 0.15). The dispersivity and diffusion coefficients were taken to be 5 cm and 0.80 cm^2 day^{-1}, respectively. Measured soil hydraulic and other properties of the five soil layers are given elsewhere (Seuntjens et al. 2002).

Results obtained with the combined HYDRUS1D-PHREEQC model will be compared in this example against results obtained with a different geochemical computer program CRUNCH. The CRUNCH model is based on the GIMRT/OS3D package of Steefel and Yabusaki (1996) and Steefel (2000). The geochemical reactions and transport in CRUNCH are coupled in one of two ways: (1) a global implicit approach (GIMRT) based on simultaneous solutions of the transport and reaction equations, or (2) an operator time-splitting approach (OS3D) for transport and reactions that is quite similar to the SNIA sequential non-iterative approach used in the combined HYDRUS1D-PHREEQC model. GIMRT generally leads to smaller numerical errors than SNIA. A comparison of HYDRUS1D-PHREEQC and CRUNCH-GIMRT allows one to assess numerical discretization errors of the SNIA coupling as a function of the maximum finite-element Courant number, C_r, which is defined as $C_r = q\Delta t/\theta\Delta x$, where Δt and Δx are temporal and spatial discretizations of the invoked numerical solution, respectively.

Figure 2 (see Color pages elsewhere in this book) shows selected results for simulations with CRUNCH-GIMRT, CRUNCH-OS3D ($Cr = 0.5$) and HYDRUS1D-PHREEQC ($Cr = 0.5$ and 0.1). Infiltration of the low-pH solution causes an increase in the number of protonated sites on the cation exchange complex (Figure 2c and d), leading to leaching of the heavy metals. Cd concentrations in the leachate from the 50-cm deep profile reach a peak after about 0.3 year (b), with most Cd leached from the profile after 1 year.

Results obtained with CRUNCH-SNIA and HYDRUS1D-PHREEQC using $C_r = 0.5$ showed very good agreement, especially for the outflow curves. The SNIA approach with $C_r = 0.5$ produced slightly more numerical dispersion as compared to simulations using the global implicit approach (CRUNCH-GIMRT), such as in the pH outflow curve, and the different profiles after 0.7 year. Reducing the Courant number to 0.1 in HYDRUS1D-

PHREEQC produced excellent agreement with CRUNCH-GIMRT.

Extension to transient variably-saturated flow

   The coupled model HYDRUS1D-PHREEQC allows one to simulate reactive transport during variably-saturated unsteady flow. Using the same soil profile data from the first example (but now assuming a fixed CEC), the transport of Na, K, Ca, Mg, Cd, Zn and Pb was simulated for a period of 8.2 year using meteorological data for the Kempen region in the northern part of Belgium from 1972 to 1981. Cumulative potential and actual net fluxes (precipitation minus potential or actual evaporation) across the soil surface are shown in Figure 3. The actual cumulative downward flux is higher than the potential flux since the sandy soil could not deliver enough water to maintain the potential evaporation rate during dry periods, thus leading to lower actual evaporation rates. In addition to the atmospheric boundary conditions, steady-state flow simulations were carried out with a constant surface flux density of 0.107 cm day^{-1}.
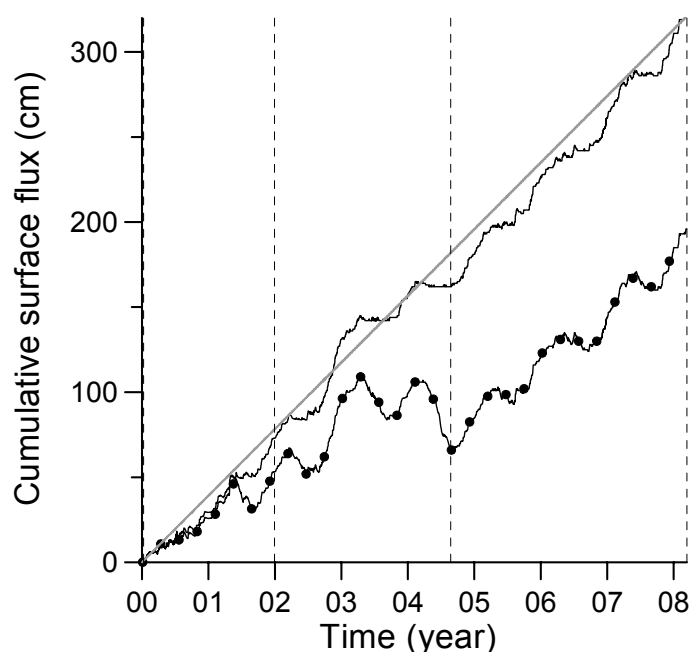
Figure 3. Atmospheric boundary conditions used for the heavy-metal transport problem. Shown are the cumulative potential (black line with dots) and actual (black line) net surface water fluxes for the transient flow simulation, and the cumulative surface flux (gray line) for the steady-state simulation

   Figure 4 shows distributions of the total concentrations C_T of Na, Ca and Cd in the top 50 cm of the layered soil profile at four times. For the steady-state simulation, Ca and Cd concentrations decreased in the top 20 cm. Cd is almost completely leached from this layer due to aqueous complexation with Cl initially present in the soil solution. The use of atmospheric boundary conditions caused less leaching of elements from the top layer, in part due to upward flow and transport during dry periods. For example, the total concentration of Na increased significantly after a long dry period at approximately 4.7 years. Because they are more strongly held on the cation exchange complex, Ca and Cd show somewhat less pronounced accumulation. The effect of using atmospheric boundary conditions was relatively large; total concentrations were up to one order of

magnitude higher than those obtained assuming steady-state flow. This result is important when, for example, simulating plant uptake of heavy metals or modeling the degradation of organic contaminants. This example shows that the coupling of HYDRUS-1D and PHREEQC leads to a potentially very powerful tool for simulating a broad range of interacting physical, chemical and biological processes affecting solute transport in soils.
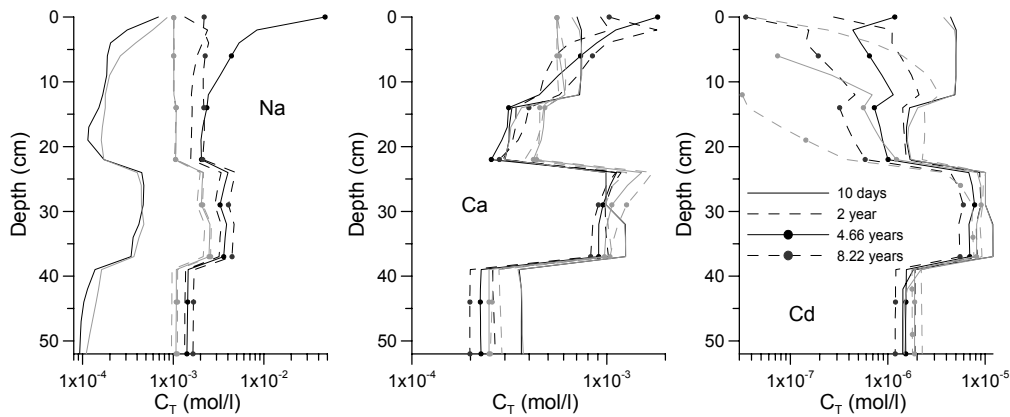
Figure 4. Distributions of the total concentration, c_T (mol/l), of Na, Ca and Cd in the top 50 cm of a physically and chemically layered soil profile at four times during steady-state (gray lines) and atmospheric (precipitation/evaporation, black lines) flow conditions

Colloid and colloid-facilitated transport

Colloids and a variety of micro-organisms (including bacteria and viruses) are subject to the same subsurface fate and transport processes as chemical compounds, while additionally being subject to their own unique complexities. For example, many colloids and microbes are negatively charged so that they are electrostatically repelled by negatively-charged solid surfaces, which may lead to an anion exclusion process causing slightly enhanced transport relative to fluid flow. Size exclusion may similarly enhance the advective transport of colloids by limiting their presence and mobility to the larger pores (e.g. Bradford et al. 2003). At the same time, colloids and biologically reactive solutes and bacteria may be subject to adsorption–desorption at solid surfaces, and accumulation at air–water interfaces, although the exact physical-chemical processes of sorption at air–water interfaces are still being debated (Thompson and Yates 1999; Wan and Tokunaga 2002; Crist et al. 2004). In addition, the transport of colloids and micro-organisms is affected by filtration and straining in the porous matrix, which is a function of the size of the colloid or micro-organism, the water-filled pore size distribution, and the pore water velocity (Elimelech and O' Melia 1990; Bradford et al. 2003; McCarthy and McKay 2004). As such, colloid and microbial biomass accumulation may also reduce the porosity of soils and alter the unsaturated soil hydraulic properties.

Additionally, inorganic, organic and microbiologically active colloids with diameters between 0.01 and 10 micrometer may enhance the transport of otherwise immobile chemicals or microbes by colloid-facilitated transport (Kretzschmar et al. 1999; Totsche and Kögel-Knabner 2004). Much evidence now exists that many contaminants are transported not only in a dissolved state by water, but also sorbed to moving colloids. Numerous examples exist in the literature illustrating this colloid-facilitated transport, including for radionuclides (Von Gunten, Waber and Krähenbühl 1988; Noell et al.

1998), pesticides (Vinten, Yaron and Nye 1983; Kan and Tomson 1990; Lindqvist and Enfield 1992), heavy metals (Grolimund et al. 1996), viruses, pharmaceuticals (Tolls 2001; Thiele-Bruhn 2003), hormones (Hanselman, Graetz and Wilkie 2003) and other contaminants (Magee, Lion and Lemley 1991; Mansfeldt et al. 2004). Many of these contaminants are normally strongly sorbed to soil and hence should not be very mobile in the subsurface. However, since they can also be sorbed to colloids which often move at rates similar as non-sorbing tracers, the potential of enhanced transport of colloid-adsorbed contaminants can be very significant.

In view of the many processes involved, numerical simulation of colloid and colloid-facilitated transport is still a major and largely unresolved challenge (De Jonge, Kjaergaard and Moldrup 2004; DeNovio, Saiers and Ryan 2004). Models not only need to describe transport, attachment, detachment, straining and/or blocking or size exclusion of colloids, but also must consider transport, reactions, and kinetic and instantaneous sorption of contaminants to both the soil and the colloids (Bradford et al. 2003; Totsche and Kögel-Knabner 2004). In this section we describe mathematical models for both colloid transport and colloid-facilitated contaminant transport. The models have recently been incorporated in the HYDRUS software packages.

Colloid transport

Colloid fate and transport models are commonly based on some form of the advection–dispersion equation, but modified to account for colloid filtration (Harvey and Garabedian 1991; Hornberger, Mills and Herman 1992; Corapcioglu and Choi 1996). In the absence of colloid inactivation and degradation, the colloid transport equation is then given by

$$\frac{\partial \theta_w C_c}{\partial t} + \frac{\partial A_{aw} \Gamma_c}{\partial t} + \rho \frac{\partial S_c}{\partial t} = \frac{\partial}{\partial x}\left(\theta_w D_c \frac{\partial C_c}{\partial x}\right) - \frac{\partial q_c C_c}{\partial x}$$

(6)

where C_c is the colloid concentration in the aqueous phase (nL^{-3}), Γ_c is the colloid concentration adsorbed to the air–water interface (nL^{-2}), S_c is the solid-phase colloid concentration (nM^{-1}), θ_w is the volumetric water content accessible to colloids (L^{3}L^{-3}) (due to ion or size exclusion, θ_w may be smaller than the total volumetric water content θ), A_{aw} is the air–water interfacial area per unit volume (L^{2}L^{-3}), D_c is the dispersion coefficient for colloids (L^{2}T^{-1}), and q_c is the volumetric water flux density for colloids (LT^{-1}). The colloid mass-transfer term between the aqueous and solid phases, E_{sw}, is traditionally given as:

$$E_{sw} = \rho \frac{\partial S_c}{\partial t} = \theta_w k_{ac} \psi_s C_c - \rho k_{dc} S_c$$

(7)

in which k_{ac} and k_{dc} are first-order colloid attachment and detachment coefficients (T^{-1}), respectively, and ψ_s is a dimensionless colloid retention function (-). The attachment coefficient is generally calculated using filtration theory (Logan et al. 1995), a quasi-empirical formulation in terms of the median grain diameter of the porous medium (often termed the collector), the pore-water velocity, and collector and collision (or sticking) efficiencies accounting for colloid removal due to diffusion, interception and gravitational sedimentation (Rajagopalan and Tien 1976; Logan et al. 1995). The first-order detachment coefficient in Eq. (7) accounts for colloid mobilization, presumably as

affected by changes in pore-water chemistry (ionic strength, ionic composition, and pH) and physical perturbations in flow, including changes in the flow rate and the water content. The attachment and detachment coefficients in (7) have been found to depend strongly upon water content, with attachment significantly increasing as the water content decreases.

To simulate reductions in the attachment coefficient due to filling of favorable sorption sites, ψ_s is sometimes assumed to decrease with increasing colloid mass retention. Random sequential adsorption (Johnson and Elimelech 1995) and Langmuirian dynamics (Adamczyk et al. 1994) equations have been proposed for ψ_s to describe this blocking phenomenon, with the latter equation given by:

$$\psi_s = 1 - \frac{S_c}{S_c^{max}}$$

(8)

in which S_c^{max} is the maximum solid-phase colloid concentration (nM^{-1}). Alternatively, blocking could possibly be described also using non-linear Freundlich sorption. Conversely, enhanced colloid retention during porous-medium ripening can theoretically be described using a functional form of ψ_s that increases with increasing mass of retained colloids. To our knowledge, no functional forms for ψ_s have been proposed to describe porous-medium ripening. We refer to several recent studies (Ginn et al. 2002; DeNovio, Saiers and Ryan 2004; Rockhold, Yarwood and Selker 2004) for more detailed discussions of the attachment and detachment coefficients in Eq. (7).

Notice that Eq. (7) lumps the effects of a variety of physical and chemical processes into a single attachment-coefficient parameter. Bradford et al. (2002; 2003) hypothesized that the influence of straining and attachment mechanisms on colloid retention should be separated into two distinct components: attachment and detachment per se, and straining (being the entrapment of colloids in pore throats that are too small to allow passage). They modeled the influence of straining using an irreversible first-order expression. In that case, E_{sw} becomes:

$$E_{sw} = \rho \frac{\partial S_c}{\partial t} = E_{sw}^{str} + E_{sw}^{att} = \rho \frac{\partial S_c^{str}}{\partial t} + \rho \frac{\partial S_c^{att}}{\partial t} =$$
$$= \theta_w \psi_s^{str} C_c k_{str} + (\theta_w \psi_s C_c k_{ac} - \rho k_{dc} S_c^{att})$$

(9)

where E_{sw}^{str} and E_{sw}^{att} are the rates of mass exchange for colloid straining and attachment/detachment (nL^{-3}T^{-1}), respectively, k_{str} is the first-order straining coefficient (T^{-1}), and S_c^{str} and S_c^{att} are the solid-phase concentrations of strained and attached colloids (nM^{-1}), respectively. The first term on the right-hand side of the above equation now accounts for straining and the second term for attachment–detachment.

Application of the first-order attachment-–detachment model given by Eq. (7) typically leads to exponential colloid distributions versus depth. Bradford et al. (2003) showed that such exponential distributions are often inconsistent with experimental data. They obtained much better results using a depth-dependent straining coefficient in Eq. (9) of the form

$$\psi_s^{str} = \left(\frac{d_{50} + z}{d_{50}} \right)^{-\beta}$$

(10)

where d_{50} is the median grain size of the porous media (L), β is a fitting parameter (-), and z is distance from the porous-medium inlet (L). Data from Bradford (2002; 2003) for different colloid diameters (d_p) and porous media median grain sizes showed an optimal value of 0.43 for β, while k_{str} could be described using a unique increasing function of the ratio of d_p/d_{50}. Subsequent studies with layered soils (Bradford et al. 2004) showed the importance of straining at and close to textural interfaces when flow occurs in the direction of coarse-textured to medium- and fine-textured media. Straining was found to be a significant mechanism for colloid retention for values of d_p/d_{50} greater than 0.005. That study also showed the importance of liquid-phase velocity distributions, colloid retention at soil textural interfaces, and size exclusion.

Finally we note that a model similar to Eq. (7) may be used to describe the partitioning of colloids to the air–water interface:

$$E_{aw} = \frac{\partial A_{aw} \Gamma_c}{\partial t} = \theta_w k_{aca} \psi_a C_c - A_{aw} k_{dca} \Gamma_c \tag{11}$$

where E_{aw} is the colloid mass-transfer term between the bulk water and the air–water interface ($nL^{-3}T^{-1}$), ψ_a is a dimensionless colloid retention function for the air–water interface (-) similarly as used in (7), and k_{aca} and k_{dca} are the first-order colloid attachment and detachment coefficients to/from the air–water interface (T^{-1}), respectively.

Colloid-facilitated solute transport

Colloid-facilitated transport requires knowledge of colloid transport, dissolved-contaminant transport, and colloid-facilitated contaminant transport. Transport and/or mass-balance equations must therefore be formulated for the total contaminant, for contaminant sorbed kinetically or instantaneously to the solid phase, and for contaminant sorbed to mobile colloids, to colloids attached to the soil solid phase, and to colloids accumulating at the air–water interface. As an illustration of the complexities involved, we review here the equations for colloid-facilitated transport that we recently incorporated in the HYDRUS software packages.

Mass-balance equation for the total contaminant. The combined dissolved and colloid-facilitated contaminant transport equation (in one dimension) is given by:

$$\frac{\partial \theta C}{\partial t} + \rho \frac{\partial S_e}{\partial t} + \rho \frac{\partial S_k}{\partial t} + \frac{\partial \theta_w C_c S_{mc}}{\partial t} + \rho \frac{\partial S_c S_{ic}}{\partial t} + \frac{\partial A_{aw} \Gamma_c S_{ac}}{\partial t} = -\frac{\partial J_T}{\partial x} - R$$

$$-\frac{\partial J_T}{\partial x} = \frac{\partial}{\partial x}\left(\theta D \frac{\partial C}{\partial x}\right) - \frac{\partial q C}{\partial x} + \frac{\partial}{\partial x}\left(\theta_w S_{mc} D_c \frac{\partial C_c}{\partial x}\right) - \frac{\partial q_c C_c S_{mc}}{\partial x} \tag{12}$$

where θ is the volumetric water content ($L^3 L^{-3}$) (note that we use the entire water content for the contaminant), C is the dissolved-contaminant concentration in the aqueous phase (ML^{-3}), S_e and S_k are contaminant concentrations sorbed instantaneously and kinetically, respectively, to the solid phase (MM^{-1}); S_{mc}, S_{ic}, and S_{ac} are contaminant concentrations sorbed to mobile and immobile (attached to solid and air–water interface) colloids (Mn^{-1}), respectively; J_T is the total flux of the dissolved contaminant ($ML^{-3}T^{-1}$), D is the dispersion coefficient for contaminants in solution (L^2T^{-1}), q is the volumetric water flux

density for the contaminant (LT^{-1}), and R represents various chemical and biological reactions, such as degradation and production ($ML^{-3}T^{-1}$), discussed below. Note that the left-hand side sums the mass of contaminant associated with the different phases (contaminant in the liquid phase, contaminant sorbed instantaneously and kinetically to the solid phase, and contaminant sorbed to mobile and immobile (attached to solid phase or air–water interface) colloids), while the right-hand side considers various spatial mass fluxes (dispersion and advective transport of the dissolved contaminant, and dispersion and advective transport of contaminant sorbed to mobile colloids).

Mass-balance equation for contaminant sorbed to the solid phase. Equation (13) invokes the concept of two-site sorption for modeling non-equilibrium adsorption–desorption reactions (e.g. Van Genuchten and Wagenet 1989). The two-site sorption concept assumes that total sorption, S, can be divided into two fractions:

$$S = S_e + S_k \tag{13}$$

with sorption S_e (MM^{-1}) on one fraction of the sites (type-1 sites) assumed to be instantaneous, and sorption S_k (MM^{-1}) on the remaining sites (type-2 sites) being time-dependent according to

$$\rho \frac{\partial S_k}{\partial t} = \theta k_{as} C - \rho k_{ds} S_k - R_s \tag{14}$$

where k_{as} is the rate of the contaminant sorption to the solid phase (type 2) (T^{-1}), k_{ds} is the rate of the contaminant desorption from the solid phase (type 2) (T^{-1}), and R_s represents various chemical and biological reactions of the kinetically sorbed contaminant ($ML^{-3}T^{-1}$).

Mass-balance equation for contaminant sorbed to mobile colloids. The mass-balance equation for contaminant sorbed to mobile colloids can be written as

$$\frac{\partial \theta_w C_c S_{mc}}{\partial t} = \frac{\partial}{\partial x}\left(\theta_w S_{mc} D_c \frac{\partial C_c}{\partial x} \right) - \frac{\partial q_c C_c S_{mc}}{\partial x} +$$
$$+\theta k_{amc}\psi_m C - \theta_w k_{dmc} C_c S_{mc} - \theta_w (k_{ac}\psi_s + k_{str}\psi_s^{str})C_c S_{mc} + \rho k_{dc} S_c^{att} S_{ic} - R_{mc} \tag{15}$$

where k_{amc} is the adsorption rate to mobile colloids (T^{-1}), k_{dmc} is the desorption rate from mobile colloids (T^{-1}), and R_{mc} represents various chemical and biological reactions for contaminant sorbed to mobile colloids ($ML^{-3}T^{-1}$). The parameter ψ_m adjusts the sorption rate to the number of mobile colloids present, i.e.,

$$\psi_m = \frac{C_c}{C_c^{ref}} \tag{16}$$

where C_c^{ref} is the reference concentration of colloids for which the sorption rate k_{amc} is valid (ML^{-3}). In equation (15), the first two terms on the right-hand side represent dispersion and advective transport, respectively, of contaminant sorbed to mobile

colloids; the third and fourth terms account for sorption and desorption of contaminants to/from mobile colloids, respectively; the fifth and sixth terms account for the attachment (including straining) and detachment of mobile colloids containing sorbed contaminants, respectively; while the seventh term represents degradation or other reactions involving contaminant sorbed to mobile colloids.

Mass-balance equation for contaminant sorbed to immobile colloids. The mass-balance equation for contaminant sorbed to immobile colloids can be written as follows

$$\rho \frac{\partial S_c S_{ic}}{\partial t} = \theta k_{aic} \psi_i C - \rho k_{dic} S_c S_{ic} + \theta_w (k_{ac} \psi_s + k_{str} \psi_s^{str}) C_c S_{mc} - \rho k_{dc} S_c^{att} S_{ic} - R_{ic} \tag{17}$$

where k_{aic} is the adsorption rate to immobile colloids (T^{-1}), k_{dic} is the desorption rate from immobile colloids (T^{-1}), and R_{ic} represents various reactions for contaminant sorbed to immobile colloids ($ML^{-3}T^{-1}$). The parameter ψ_i adjusts the sorption rate to the number of immobile colloids present:

$$\psi_i = \frac{S_c}{S_c^{ref}} \tag{18}$$

where S_c^{ref} is the reference concentration of immobile colloids for which the sorption rate k_{aic} is valid (ML^{-3}). In equation (17) the first two terms on the right-hand side represent adsorption and desorption of contaminant to/from immobile colloids, respectively; the third and fourth terms describe the attachment (including straining) and detachment of immobile colloids with sorbed contaminant, respectively; and the fifth term represents reactions of contaminant sorbed to immobile colloids.

Mass-balance equation for contaminant sorbed to colloids attached to the air–water interface. The mass-balance equation for contaminant sorbed to colloids attached to the air–water interface may be written as

$$\frac{\partial A_{aw} \Gamma_c S_{ac}}{\partial t} = \theta k_{aac} \psi_g C - A_{aw} k_{dac} \Gamma_c S_{ac} + \theta_w k_{acd} \psi_a C_c S_{mc} - A_{aw} k_{dca} \Gamma_c S_{ac} - R_{ac} \tag{19}$$

where k_{aac} is the adsorption rate to colloids at the air–water interface (T^{-1}), k_{dac} is the desorption rate from colloids at the air–water interface (T^{-1}), and R_{ac} represents various reactions for contaminant sorbed to colloids at the air–water interface ($ML^{-3}T^{-1}$). Similarly as in (17), the parameter ψ_g adjusts the sorption rate to the number of colloids at the air–water interface:

$$\psi_g = \frac{\Gamma_c}{\Gamma_c^{ref}} \tag{20}$$

where Γ_c^{ref} is the reference concentration of immobile colloids for which sorption rate k_{aic} is valid (ML^{-3}). In equation (19) the first two terms on the right-hand side represent the sorption and desorption, respectively, of contaminant to/from colloids at the air–water interface; the third and fourth terms account for the attachment and detachment,

respectively, of colloids with sorbed contaminant to/from the air–water interface; whereas the fifth term represents degradation and other reactions of contaminant sorbed to colloids accumulated at the air–water interface.

Reaction term. The reaction term R in (12) may be used to account for a variety of chemical and biological reactions and transformations, including degradation and production, not already explicitly incorporated in the main total contaminant mass-transport equation. Consistent with current capabilities of the HYDRUS software packages (Šimůnek, Šejna and Van Genuchten 1998; 1999) to simulate sequential first-order decay chains, R may include provisions for two first-order degradation reactions: one which is independent of other solutes and one which provides the coupling between solutes involved in sequential first-order decay reactions. As discussed earlier in Section 2, problems of solute transport involving sequential first-order decay reactions frequently occur in soil and groundwater systems. The reaction term R in (12) for colloid-facilitated transport scenarios is now given by:

$$R = -(\mu_w + \mu_w')\theta C - (\mu_s + \mu_s')\rho_b(S_e + S_k) - (\mu_c + \mu_c')(\theta_w C_c S_{mc} + \rho S_c S_{ic} +$$
$$A_{aw}\Gamma_c S_{ac}) + \mu_w^{'*}\theta C^* + \mu_s^{'*}\rho(S_e^* + S_k^*) + \mu_c^{'*}(\theta_w C_c S_{mc}^* + \rho S_c S_{ic}^* + A_{aw}\Gamma_c S_{ac}^*) \quad (21)$$

where μ_w, μ_s, and μ_c are first-order rate constants (T^{-1}) for solutes in the liquid, solid and colloid phases (T^{-1}), respectively; μ_w', μ_s', and μ_c' are similar first-order rate constants (T^{-1}) providing connections between individual chain species, and terms with the superscript * belong to solutes preceding in the chain reaction. The reaction terms R_s, R_m, R_{im}, and R_a for reactions in the kinetically sorbed phase, on mobile colloids and on colloids associated either with the solid phase or the air–water interface, respectively, are as follows:

$$R_s = -(\mu_s + \mu_s')\rho S_k + \mu_s^{'*}\rho S_k^*$$
$$R_{mc} = -(\mu_s + \mu_s')\theta_w C_c S_{mc} + \mu_c^{'*}\theta_w C_c S_{mc}^*$$
$$R_{ic} = -(\mu_c + \mu_c')\rho S_c S_{ic} + \mu_c^{'*}\rho S_c S_{ic}^*$$
$$R_{ac} = -(\mu_c + \mu_c')A_{aw}\Gamma_c S_{ac} + \mu_c^{'*}A_{aw}\Gamma_c S_{ac}^* \quad (22)$$

The above mathematical development shows that a complete description of colloid-facilitated transport requires a total of nine coupled partial differential equations involving nine unknown variables (C_c, S_c^{str}, S_c^{att}, Γ_c, C, S_k, S_{mc}, S_{ic}, S_{ac}).

Example application for colloid-facilitated transport

Typical features of colloid and colloid-facilitated transport are demonstrated here for a hypothetical column experiment. The column was assumed to have a length, L, of 10 cm, while the experiment lasted 600 minutes. Water flowed through the column at full saturation (the saturated water content was equal to 0.50) at a flux density, q, of 0.1 cm min^{-1}. Both colloids and the contaminant were assumed to be applied at unit (relative) concentrations at the top of the column during a time period of 60 min. The soil bulk density, ρ, was set equal to 1.5 g cm^{-3}, while the dispersivity, λ, for both the colloids and the contaminant was assumed to be 0.1 cm. The colloid attachment and detachment coefficients, k_a and k_d, were taken to be 0.01 and 0.005 min^{-1}, respectively. Solute

sorption to soil was considered instantaneous with the distribution coefficient, K_d, equal to 2 L kg^{-1}. Solute adsorption was assumed to be the same for both the mobile and immobile colloids, but with different rate coefficients of $k_{amc}= k_{aic}=0.1$ min^{-1} and $k_{dmc}= k_{dic}=0.02$ min^{-1}, respectively, and with $C_c^{ref}= S_c^{ref}=1$. For these conditions, one pore volume, T, is equal to 50 minutes [$t = TL/v = TL\theta_s/q = 1 * (10$ cm$) * 0.5 / (0.1$ cm/min$) = 50$ min], while the retardation factor for the contaminant equals 7 ($R = 1 + \rho K_d/\theta_s = 1 + 1.5*2/0.5 = 7$).

Figure 5 shows colloid and total solute concentrations at depths of 5 and 10 cm. The main concentration fronts for both colloids and solute arrived, as expected, at 1 and 7 pore volumes (i.e., after 50 and 350 minutes), respectively. However, a significant amount of solute arrived much earlier than at 7 pore volumes. This earlier arrival is due to the accelerated movement of solute sorbed to mobile colloids.

Figure 6 presents colloid and solute fluxes at the bottom of the column. Notice that the solute flux (Figure 6b) has two concentration peaks. The first peak corresponds to contaminant arriving sorbed to colloids, which have a retardation factor, R, equal to 1 (no sorption or anion exclusion), while the second peak corresponds to solute arriving dissolved in water ($R=7$, $t=350$ min). Also notice that the initial contaminant fluxes (Figure 6b) are smaller relative than the colloid fluxes, which show a plateau of certain duration. This is because contaminant sorption onto the colloids was assumed to be a kinetic process which requires a certain time period for sorption to be complete. The contaminant flux for this reason keeps increasing until it suddenly drops at the end of the colloid pulse. Hence, the largest contaminant fluxes during the first peak occurred just before the end of the colloid pulse (Figure 6b). Colloids keep arriving at the bottom of the column after the main colloid pulse due to kinetic colloid detachment from the solid phase (Figure 6a). By comparison, considerable solute fluxes are present between the two solute peaks as a result of solute both sorbed to colloids and, increasingly, dissolved in water. The dissolved solute fluxes at the end of the column were initially also due to enhanced transport by the colloids in especially the upper part of the columns, and subsequent desorption into the liquid phase (Figure 6b). As expected, the bulk of the contaminant arrived at approximately 350 minutes, consistent with a solute retardation factor, R, of 7.
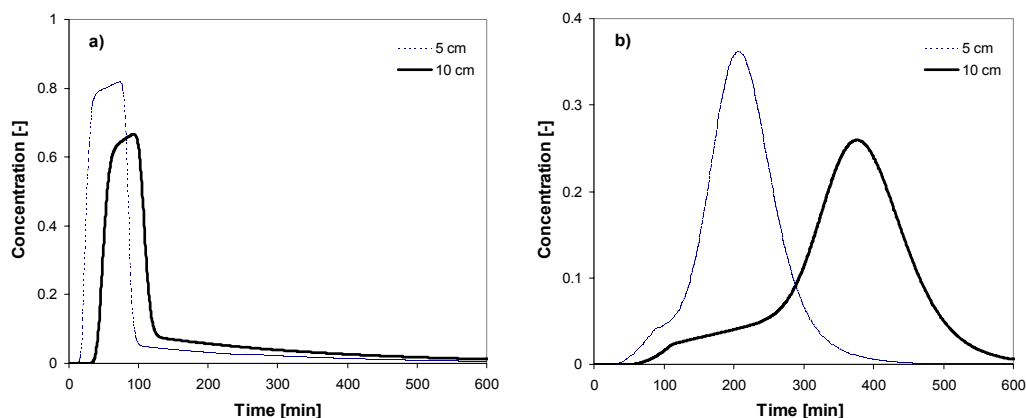
Figure 5. Colloid (a) and contaminant (b) concentrations at a depth of 5 and 10 cm
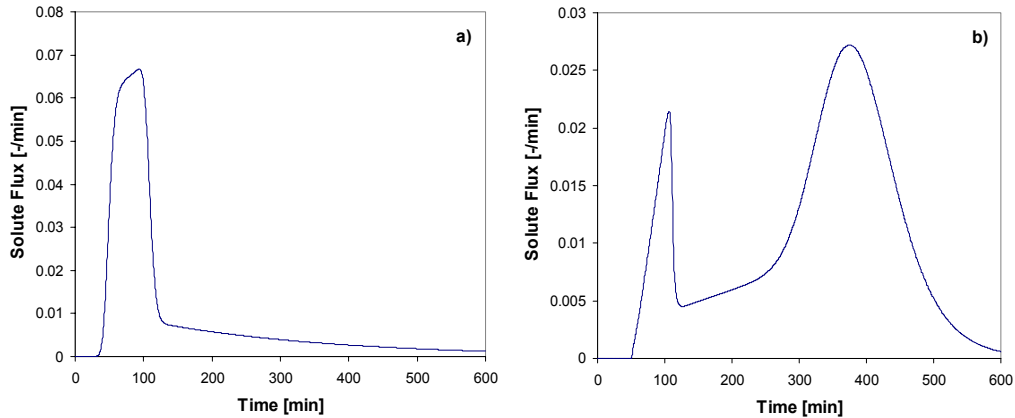
Figure 6. Calculated colloid (a) and contaminant (b) flux densities at the bottom of the 10-cm-long soil column

Coupled surface – subsurface flow

Much progress has been made over the years also in modeling various components of overland flow and variably-saturated subsurface flow. Traditionally, however, surface and subsurface flow processes have been considered mostly separately, with some of the processes being severely simplified when coupled surface and subsurface flow was simulated. For example, existing surface irrigation models typically still use empirical infiltration functions such as the Philip, Kostiakov, modified Kostiakov, and Branch infiltration equations (e.g. Woolhiser, Smith and Goodrich 1990; Strelkoff, Clemmens and Schmidt 1998), rather than rigorously simulating subsurface water flow and solute transport using the Richards equation for variably-saturated flow, and advection–dispersion equations for solute transport. Several weakly coupled, mostly iterative or time-lagged approaches using the Richards equation have been pursued for larger-scale surface runoff or small watershed-scale applications. Early examples are given by Zhang and Cundy (1989) and Govindaraju and Kavvas (1991). Still, because of a lack of tight (numerically implicit) coupling between the surface and subsurface flow and transport processes, previous models have not proven reliable for untested management practices under surface-irrigated conditions, nor have they been applied to linked scenarios involving surface irrigation, chemical runoff, deep drainage, solute leaching and crop growth.

Recently, several more integrated approaches have been proposed. The first and probably still the most comprehensive integrated physically-based model was formulated by VanderKwaak (1999). This model included most or all known stream-flow generation mechanisms, variably-saturated subsurface flow, advective–dispersive solute transport in both surface and subsurface flow, and provisions for preferential flow within vadose-zone fractures and macropores. The surface and subsurface components were linked using first-order flux relationships such that one set of discrete algebraic expressions resulted from the fully-coupled numerical approach. The model was applied to a small watershed in Canada (VanderKwaak 1999), as well as to a well-studied catchment in Oklahoma (VanderKwaak and Loague 2001). Panday and Huyakorn (2004) proposed a similar fully-coupled spatially-distributed model for conjunctive surface/subsurface flow involving three-dimensional variably-saturated subsurface flow, two-dimensional overland flow, and one-dimensional flow through such surface structures as rivers and canals, among other processes. Another recent example of fully coupled variably-

saturated flow and surface runoff is given by Beaugendre et al. (in prep.).

The two-dimensional illustrative example application considered here pertains to hill-slope hydrology. Water flow and solute transport in and along hill slopes is a relatively complex nonlinear problem. Rainfall water will infiltrate into the soil profile at a rate equal to the rainfall rate until the soil infiltration capacity is reached. Surface runoff will be generated once the soil infiltration capacity is exceeded. This surface runoff will redistribute water along the land surface by moving it to lower parts of the hill slope where it can infiltrate if locally enough infiltration capacity is present. As more water infiltrates in the lower part of the hill slope, more water will be available there for vegetation. More vegetation will generally result in more roots which, in turn, may enrich soil with organic matter, thus improving soil structure and further increasing the hydraulic conductivity and the infiltration capacity (Mattson et al. 2004). We are not aware of existing vadose-zone flow/transport models that describe this dynamic interaction between overland flow, subsurface infiltration and plant growth.

Governing equations

Hortonian overland flow is usually described using kinematic wave equations, which are simplifications of the Saint Venant equations and provide excellent approximations for most overland flow conditions (Woolhiser and Liggett 1967; Morris and Woolhiser 1980; Woolhiser, Smith and Goodrich 1990):

$$\frac{\partial h}{\partial t} + \frac{\partial Q}{\partial x} = q(x,t)$$

(23)

where h is the unit storage of water (or mean depth for smooth surfaces) (L), Q is the discharge per unit width ($L^2 T^{-1}$), t is time (T), x is the distance co-ordinate over the soil surface (L), and $q(x,t)$ is the rate of local input, or lateral inflow (i.e., local precipitation minus local infiltration) (LT^{-1}).

The discharge Q per unit width can be calculated as follows:

$$Q = \alpha h^m$$

(24)

where α ($L^{2-m} T^{-1}$) and m (-) are parameters related to slope, surface roughness and flow conditions (laminar or turbulent flow). The parameter α is usually evaluated using the Manning hydraulic resistance law

$$\alpha = k_0 \frac{S_m^{1/2}}{n} \qquad \text{and} \qquad m = 5/3$$

(25)

where S_m is the slope [-], k_0 is an empirical constant ($L^{1/3} T^{-1}$) equal to 1.49 $cm^{1/3}$ s^{-1}, and n is Manning's roughness coefficient for overland flow (-).

The rate of local input $q(x,t)$ in (23) integrates various inputs and outputs such as precipitation, evaporation and infiltration. Models that rigorously evaluate these components, such as the HYDRUS codes, should be ideal tools for calculating $q(x,t)$. By substituting (24) into (23) we obtain:

$$\frac{\partial h}{\partial t} + \frac{\partial \alpha h^m}{\partial x} = q(x,t) \tag{26}$$

or

$$\frac{\partial h}{\partial t} + \alpha m h^{m-1} \frac{\partial h}{\partial x} = q(x,t) \tag{27}$$

The above equations were solved using a numerically stable fully implicit four-point finite-difference method, similar to the one used in the KINEROS model (Woolhiser, Smith and Goodrich 1990). This numerical solution of the overland equation was subsequently coupled to the HYDRUS-2D computation module (Šimůnek, Šejna and Van Genuchten 1999) using transient atmospheric boundary conditions.

Example application

We used the tightly coupled overland and subsurface flow approach as incorporated into HYDRUS-2D to simulate surface runoff from a rainfall event of limited duration over a 100-m heterogeneous hill slope. The example considers surface runoff generated by a 10-minute high-intensity rainstorm (0.00667 cm s^{-1} or 24 cm h^{-1}) covering the entire hill slope. The hill slope is assumed to consist of two soil materials. The soil in the middle third of the hillside transect (between 33 and 66 m) is assumed to have a saturated hydraulic conductivity (K_s= 0.0289 cm s^{-1} or 25 m d^{-1}) that is two orders of magnitude higher than that of the other parts of the hill slope (K_s= 0.000289 cm s^{-1} or 25 cm d^{-1}). Because of this, the middle section can accommodate the infiltration of water from both rainfall itself and from runoff coming from the upgradient part of the hill slope. The soil transect has a slope of 0.01, while the roughness coefficient n was assumed to be equal to 0.01.

Figure 7 shows the depth of the water layer that develops on top of the soil surface (see Color pages elsewhere in this book). The figure also shows the steady-state water layer calculated using the analytical solution of Eq. (26) assuming no infiltration (i.e., $q = q_0$ = 24 cm h^{-1}):

$$h(x) = \left(\frac{n q_0 x}{k_0 S_m^{1/2}} \right)^{3/5} \tag{28}$$

The figure shows both the buildup and recession of the water layer along the hill slope at various times. Actual and cumulative surface runoff fluxes from the bottom of the hill slope transect, the cumulative effective rain on the transect (rainfall minus infiltration), and the volume of water in the surface layer for a 10-minute rain storm are shown in Figure 8 (see Color pages elsewhere in this book). Notice that a nearly steady-state situation for overland flow had developed at the end of the rainfall event.

Finally, Figure 9 shows contours of the water content in the soil profile 6 min after initiation of the rainfall event (see Color pages elsewhere in this book). Figure 9, as well as Figure 7, clearly shows that runoff generated in the upper third of the hillside transect moves to and infiltrates in the upper part of the middle section containing more permeable soil, and that runoff is generated again in the lower one third of the hill slope. The example demonstrates the potential of tightly coupled surface/subsurface flow models.

Preferential flow

A major challenge in dealing with the vadose zone, both in terms of modeling and experimentation, is its overwhelming heterogeneity. One manifestation of heterogeneity at intermediate spatial scales involves the preferential movement of water and chemicals through soil macropores or rock fractures. In structured or macroporous soils, water may move preferentially through large interaggregate pores, decayed root channels, and earthworm burrows, as well as through drying cracks in fine-textured soils, thereby bypassing much of the soil matrix. Preferential flow may also occur in the form of unstable flow (fingering) induced by soil textural layering, water repellency and/or air entrapment. In unsaturated fractured rock, water may similarly move preferentially through fractures and fissures, thus bypassing much of the rock matrix. Preferential flow may be caused also by funneling of water through high-conductivity layers, and/or by being redirected by sloping less-permeable layers. We refer to several recent reviews and other papers for detailed discussions of the various processes and conditions leading to preferential flow (Ritsema et al. 1993; De Rooij 2000; Evans, Nicholson and Rasmusson 2001; National Research Council 2001; Bodvarsson, Ho and Robinson 2003; Šimůnek et al. 2003; Wang et al. 2004).

An impressive array of models have been developed over the years in attempts to parameterize preferential-flow processes. While not all-inclusive, Figure 10 provides a useful schematic of increasingly complex models that have been used to simulate preferential-flow processes. Figure 10a represents the traditional case of uniform (equilibrium) flow and transport, assuming applicability of an equivalent-continuum approach based on the Richards equation (Eq. 1) for variably-saturated flow and Eq. (3) for advective–dispersive solute transport. The simplest situation for apparent preferential flow arises when the Richards and advection–dispersion equations are still used in an equivalent matrix and fracture-continuum approach, but now with composite hydraulic conductivity (permeability) curves, $K(h)$, of the type shown in Figure 10b. While still leading to uniform flow, models using such composite hydraulic properties do allow for faster flow and transport during conditions near saturation, and as such may provide more realistic simulations of field data (e.g. Peters and Klavetter 1988; Mohanty et al. 1997; 1998; Zurmühl and Durner 1996; De Vos et al. 1999).

The two parts of the conductivity curves in Figures 10b and 11a may be associated with soil structure (near saturation) and soil texture (at lower negative pressure heads). This conceptualization of $K(h)$ is consistent with analyses by Schaap and Leij (2000) of the UNSODA soil hydraulic data base (Leij et al. 1996), which show that the ratio of the measured (K_s) and extrapolated (K_{ms}) values of the hydraulic conductivity is about one order of magnitude (K_{ms} would be the value of K_s when no macropores or fractures were present). We note that the use of composite hydraulic functions that lump the effects of matrix and fracture flow into one equation, in conjunction with the Richards equation, will still lead to uniform flow, and as such cannot reproduce non-uniform moisture distributions typical of preferential flow. Still deconvolution of bimodal conductivity functions like those shown in Figure 11a may provide important information for dual-permeability models that consider separate flow domains for the fractures and matrix.

REPRESENTATION

RELATIVE PERMEABILITY CURVES

Equivalent Single Continuum

EQUIVALENT
POROUS MEDIUM

Equivalent
Porous Medium

Relative Permeability

Pressure Head

**Equivalent Matrix
and Fracture Continuum**

COMPOSITE POROSITY
(EQUIVALENT
CONTINUUM)

Equivalent Matrix
and Fracture Continuum

Matrix   Fracture
Continuum   Continuum

DUAL
POROSITY

Fracture
Continuum

Matrix   Fracture
Continuum   Continuum

DUAL
PERMEABILITY

Fracture
Continuum
Matrix
Continuum

DISCRETE FRACTURES
WITHOUT MATRIX

Fractures 1-n

DISCRETE FRACTURES
WITH MATRIX

Fractures 1-n

Matrix

Figure 10. Alternative conceptual models for flow through variably-saturated structured media (after Altman et al. 1996)

Non-uniform flow can be generated numerically only using dual-porosity or dual-permeability models for structured media, or using alternative formulations specifically derived for unstable flow (De Rooij 2000; Eliassi and Glass 2002; Dautov et al. 2002). Dual-porosity and dual-permeability models typically assume that the medium consists of two interacting pore regions, one associated with the macropore or fracture network, and one with the micropores inside soil aggregates or rock matrix blocks. Different formulations arise depending upon how water and solute movement in the micropore region is modeled, and how water and solutes between the micropore and macropore regions are allowed to interact.
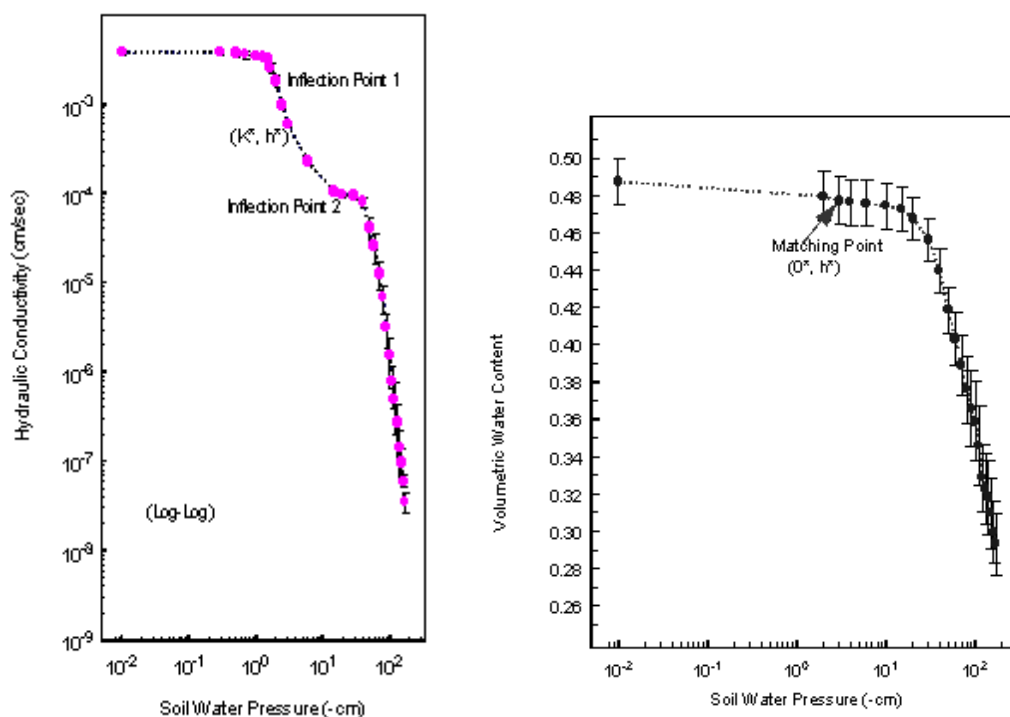
Figure 11. Plots of (a) the field-averaged hydraulic-conductivity function (geometric means and standard errors, left) and (b) the field-averaged soil water retention function (arithmetic means and standard errors) for the surface horizon at the Las Nutrias experimental site (after Mohanty et al. 1997)

Dual-porosity type models are obtained when the liquid phase is partitioned into mobile (fracture) and immobile (matrix) liquid pore regions, with water and/or solutes allowed to exchange between the two liquid regions (Figure 10c). Such models can be made quite general by permitting transient variably-saturated flow in the fracture, and simultaneously allowing water to exchange between the fracture and matrix domains (Šimůnek et al. 2003). The latter dual-porosity situation would lead to both advective and diffusive exchange of solutes between the fracture and matrix regions, but still without vertical flow in the matrix region. Popular early conceptualizations of the dual-porosity approach, when applied to solute transport only, are two-region or mobile–immobile water models (e.g. Van Genuchten and Wierenga 1976), in which solute exchange is described using first-order mass-transfer equations.

More complex dual-permeability models (Figure 10d) arise when water flow occurs in both the fracture and matrix domains. Examples of dual-permeability models are given by Gerke and van Genuchten (1993; 1996), Pruess (1991), Jarvis (1998), Liu, Doughty and Bodvarsson (1998) and Liu, Zhang and Bodvarsson (2003), among many others. These models all use different formulations for the exchange of water between the fracture and matrix regions. A summary of various exchange (mass transfer) terms for dual-porosity and dual-permeability models is given by Šimůnek et al. (2003). We note that in some dual-permeability models (e.g. Hutson and Wagenet 1995; Wilson, Jardine and Gwo 1992) more than two domains are considered, all having their unique hydraulic properties.

The modeling approach can be further refined by considering transient variably-saturated flow and/or transport in discrete well-defined macropores or fractures, either

without (Figure 10e) or with (Figure 10f) interactions between the fracture and matrix domains. The approach typically assumes that the flow and transport equations of the macropore or fracture network of prescribed geometry can be solved simultaneously and in a fully-coupled fashion with the corresponding equations for the porous matrix. Discrete-fracture models of this type (Figure 10f) are given by Shikaze, Sudicky and Mendoza (1994) for two-dimensional gas-phase flow and transport through a network of vadose-zone fractures embedded in a variably-saturated matrix, and by Therrien and Sudicky (1996) and VanderKwaak (1999) for more general three-dimensional conditions in which the Richards equation is applied both along a network of interconnected fracture planes and in the adjoining porous matrix. Discrete fracture network models are likely unfeasible for most or practical applications problems because of limited data availability and computational difficulties (Liu, Zhang and Bodvarsson 2003).

Except for the discrete fracture models, all of the models schematically shown in Figure 10 were recently incorporated in the HYDRUS-1D and HYDRUS-2D software packages (Šimůnek et al. 2003), including the use of composite soil water retention and hydraulic conductivity functions based on the formulation of Durner (1994). Additionally, we incorporated into the HYDRUS codes a dual-permeability approach using the kinematic wave equation for flow in the macropores (Jarvis 1998), as well as a relatively simple empirical but still very effective single-porosity non-equilibrium model proposed by Ross and Smettem (2000) to account for time-dependent water-content equilibration at a given pressure head [a related more process-based approach involving dynamic pressure-head equilibration is given by Hassanizadeh, Celia and Dahle (2002)]. Because of the large number of features now included in the updated HYDRUS models, we believe that the resulting codes provide great flexibility in addressing a large number of practical field-scale vadose-zone flow and transport problems involving both uniform and preferential flow (Šimůnek et al. 2003; Zhang, Šimůnek and Bowman 2004).

Concluding remarks

The topics reviewed in this paper reflect the tremendous advances that have been made during the past several decades in our ability to describe water and solute transport processes in the subsurface mathematically. Within the context of our own work, we reviewed relatively standard approaches for modeling flow and transport, and additionally ongoing research on (1) multicomponent geochemical transport, (2) colloid and colloid-facilitated transport, (3) integrated surface/subsurface modeling, and (4) process-based descriptions of preferential flow.

Continued progress in the above four areas of research requires significant advances in both numerical modeling and the underlying science. Of the four topics, we believe that the main challenges with multicomponent transport modeling and integrated surface/subsurface flow/transport modeling are first and foremost numerical in terms of coupling processes that have for too long been addressed in separate efforts. Still, formidable challenges remain here. For example, numerical algorithms and databases for multicomponent transport models must be extended to higher temperatures and ionic strengths, complex contaminant mixtures (including especially mixed organic and inorganic wastes), multiphase flow, redox disequilibria for low-temperature systems, and coupled physico-chemical systems to account for possible changes in the soil water retention and hydraulic-conductivity functions. Integrated surface/subsurface numerical models require further research on such issues as spatial and temporal scaling of hydrological, chemical and biological processes and properties, linking constitutive (soil-

hydraulic) relationships to the measurements scale, preferential flow, and issues of parameter and model uncertainty. Many of these and related specific challenges in vadose-zone research are discussed as part of a recent Department of Energy National Roadmap for Vadose Zone Science and Technology (Stephens et al. 2002; U.S. Department of Energy 2001).

By comparison, we believe that the basic scientific issues related to colloid and colloid-facilitated transport are still largely unresolved, and that our understanding here lags far behind current numerical capabilities. Much work is needed to better understand the processes of filtration, straining, size exclusion, and mobilization of colloids and micro-organisms; accumulation at air–water interfaces, interactions between micro-organisms and contaminants (including biodegradation), the effects of both physical factors (water content, flow velocity, textural interfaces) and chemical processes (ionic strength, solution composition, pH) on colloid retention and mobilization, and modeling colloid-facilitated transport during conditions of transient flow. Addressing preferential flow phenomena, and the related more general problems of subsurface heterogeneity, poses equally important challenges, as well as enormous opportunities, since those problems are at the center of many of the unresolved issues in other areas of vadose-zone flow and transport research.

Acknowledgments

References

Abrams, R.H., Loague, K. and Kent, D.B., 1998. Development and testing of a compartmentalized reaction network model for redox zones in contaminated aquifers. *Water Resources Research,* 34 (6), 1531-1541.

Adamczyk, Z., Siwek, B., Zembala, M., et al., 1994. Kinetics of localized adsorption of colloid particles. *Advances in Colloid and Interface Science,* 48, 151-280.

Ahuja, L.R., Rojas, K.W., Hanson, J.D., et al., 1999. *Root zone water quality mode: modeling management effects on water quality and crop production*. Water Resources Publications, Highlands Ranch.

Altman, S.J., Arnold, B.W., Ho, C.K., et al., 1996. *Flow calculations for Yucca Mountain groundwater travel time (GWTT-95)*. Sandia National Laboratories, Albuquerque. Report no. SAND96-0819.

Appelo, C.A.J., Verweij, E. and Schafer, H., 1998. A hydrogeochemical transport model for an oxidation experiment with pyrite/calcite/exchangers/organic matter containing sand. *Applied Geochemistry,* 13 (2), 257-268.

Beaugendre, H., Ern, E., Escaffer, T., et al., in prep. Numerical investigation of surface runoff in hillslopes with variably-saturated flows. *In:* Neittaanmäki, P., Rossi, T., Majava, K., et al. eds. *Proceedings of the European congress on computational methods in applied sciences and engineering, ECCOMAS 2004, Jyväskylä, July 24-28, 2004.*

Bell, L.S.J. and Binning, P.J., 2004. A split operator approach to reactive transport with the forward particle tracking Eulerian-Lagrangian localized adjoint method. *Advances in Water Resources,* 27 (4), 323-334.

Bodvarsson, G.S., Ho, C.K. and Robinson, B.A. (eds.), 2003. *Yucca Mountain Project.* Journal of Contaminant Hydrology, 62/63(special issue).

Bradford, S.A., Bettahar, M., Šimůnek, J., et al., 2004. Straining and attachment of colloids in physically heterogeneous porous media. *Vadose Zone Journal,* 3 (2), 384-394. [http://vzj.scijournals.org/cgi/content/full/3/2/384]

Bradford, S.A., Šimůnek, J., Bettahar, M., et al., 2003. Modeling colloid attachment, straining, and exclusion in saturated porous media. *Environmental Science and Technology,* 37 (10), 2242-2250.

Bradford, S.A., Yates, S.R., Bettahar, M., et al., 2002. Physical factors affecting the transport and fate of colloids in saturated porous media. *Water Resources Research,* 38 (12), 631-6312.

Bromilow, R.H. and Leistra, M., 1980. Measured and simulated behaviour of aldicarb and its oxidation products in fallow soils. *Pesticide Science,* 11 (4), 389-395.

Carrayrou, J., Mose, R. and Behra, P., 2004. Operator-splitting procedures for reactive transport and comparison of mass balance errors. *Journal of Contaminant Hydrology,* 68 (3/4), 239-268.

Casey, F.X.M., Hakk, H., Šimůnek, J., et al., 2004. Fate and transport of testosterone in agricultural soils. *Environmental Science and Technology,* 38 (3), 790-798.

Casey, F.X.M. and Šimůnek, J., 2001. Inverse analyses of transport of chlorinated hydrocarbons subject to sequential transformation reactions. *Journal of Environmental Quality,* 30 (4), 1354-1360.

Casey, F.X.M., Larsen, G.L., Hakk, H., et al., 2003. Fate and transport of 17[beta]-estradiol in soil-water systems. *Environmental Science and Technology,* 37 (11), 2400-2409.

Castro, C.L. and Rolston, D.E., 1977. Organic phosphate transport and hydrolysis in soil: theoretical and experimental evaluation. *Soil Science Society of America Journal,* 41 (6), 1085-1092.

Corapcioglu, M.Y. and Choi, H., 1996. Modeling colloid transport in unsaturated porous media and validation with laboratory column data. *Water Resources Research,* 32 (12), 3437-3449.

Cressey, G.B., 1958. Qanats, karez, and foggaras. *The Geographical Review,* 48, 27-44.

Crist, J.T., McCarthy, J.F., Zevi, Y., et al., 2004. Pore-scale visualization of colloid transport and retention in partly saturated porous media. *Vadose Zone Journal,* 3 (2), 444-450. [http://vzj.scijournals.org/cgi/content/full/3/2/444]

Darcy, H., 1856. *Les fontaines publiques de la ville de Dyon.* Dalmont, Paris.

Dautov, R.Z., Egorov, A.G., Nieber, J.L., et al., 2002. Simulation of two-dimensional gravity-driven unstable flow. *In:* Hassanizadeh, S.M., Schotting, R.J., Gray, W.G., et al. eds. *Computational methods in water resources: proceedings of the XIVth international conference on computational methods in water resources (CMWR XIV), June 23-28, 2002, Delft, The Netherlands. Volume 1.* Elsevier, Amsterdam, 9-16. Developments in Water Science no. 47.

De Jonge, L.W., Kjaergaard, C. and Moldrup, P., 2004. Colloids and colloid-facilitated transport of contaminants in soils: an introduction. *Vadose Zone Journal,* 3 (2), 321-325. [http://vzj.scijournals.org/cgi/content/full/3/2/321]

De Rooij, G.H., 2000. Modeling fingered flow of water in soils owing to wetting front instability: a review. *Journal of Hydrology,* 231/232, 277-294.

De Vos, J.A., Šimůnek, J., Raats, P.A.C., et al., 1999. Identification of the hydraulic characteristics of a layered silt loam soil. *In:* Van Genuchten, M.T., Leij, F.J. and Wu, L. eds. *Characterisation and measurement of the hydraulic properties of unsaturated porous media: proceedings of the international workshop. Part 1.* University of California, Riverside, 783-798.

DeNovio, N.M., Saiers, J.E. and Ryan, J.N., 2004. Colloid movement in unsaturated porous media: recent advances and future directions. *Vadose Zone Journal,* 3 (2), 338-351. [http://vzj.scijournals.org/cgi/content/full/3/2/338]

Durner, W., 1994. Hydraulic conductivity estimation for soils with heterogeneous pore structure. *Water Resources Research,* 30 (2), 211-223.

Dutt, G.R., Shaffer, M.J. and Moore, W.J., 1972. *Computer simulation model of dynamic bio-physicochemical processes in soils.* University of Arizona, Tucson. Technical bulletin / Department of Soils, Water and Engineering, University of Arizona no. 196.

Eliassi, M. and Glass, R.J., 2002. On the porous-continuum modeling of gravity-driven fingers in unsaturated materials: extension of standard theory with a hold-back-pile-up effect. *Water Resources Research,* 38 (11), 161-1611.

Elimelech, M. and O' Melia, C.R., 1990. Kinetics of deposition of colloidal particles in porous media. *Environmental Science and Technology,* 24 (10), 1528-1536.

Essaid, H.I., Bekins, B.A., Godsy, E.M., et al., 1995. Simulation of aerobic and anaerobic biodegradation processes at a crude oil spill site. *Water Resources Research,* 31 (12), 3309-3327.

Evans, D.D., Nicholson, T.J. and Rasmusson, T.C. (eds.), 2001. *Flow and transport through unsaturated fractured rock.* 2nd edn. American Geophysical Union, Washington. Geophysical Monograph no. 42.

Fryar, A.E. and Schwartz, F.W., 1994. Modeling the removal of metals from groundwater by a reactive barrier: experimental results. *Water Resources Research,* 30 (12), 3455-3469.

Gerke, H.H. and Van Genuchten, M.T., 1993. A dual-porosity model for simulating the preferential movement of water and solutes in structured porous media. *Water Resources Research,* 29 (2), 305-319.

Gerke, H.H. and Van Genuchten, M.T., 1996. Macroscopic representation of structural geometry for simulating water and solute movement in dual-porosity media. *Advances in Water Resources,* 19 (6), 343-357.

Ginn, T.R., Wood, B.D., Nelson, K.E., et al., 2002. Processes in microbial transport in the natural subsurface. *Advances in Water Resources,* 25 (8/12), 1017-1042.

Govindaraju, R.S. and Kavvas, M.L., 1991. Dynamics of moving boundary overland flows over infiltrating surfaces at hillslopes. *Water Resources Research,* 27 (8), 1885-1898.

Grolimund, D., Borkovec, M., Barmettler, K., et al., 1996. Colloid-facilitated transport of strongly sorbing contaminants in natural porous media: a laboratory column study. *Environmental Science and Technology,* 30 (10), 3118-3123.

Hanselman, T.A., Graetz, D.A. and Wilkie, A.C., 2003. Manure-borne estrogens as potential environmental contaminants: a review. *Environmental Science and Technology,* 37 (24), 5471-5478.

Harvey, R.W. and Garabedian, S.P., 1991. Use of colloid filtration theory in modeling movement of bacteria through a contaminated sandy aquifer. *Environmental Science and Technology,* 25 (1), 178-185.

Hassanizadeh, S.M., Celia, M.A. and Dahle, H.K., 2002. Dynamic effect in the capillary

pressure-saturation relationship and its impacts on unsaturated flow. *Vadose Zone Journal,* 1 (1), 38-57. [http://vzj.scijournals.org/cgi/content/full/1/1/38]

Hornberger, G.M., Mills, A.L. and Herman, J.S., 1992. Bacterial transport in porous media: evaluation of a model using laboratory observations. *Water Resources Research,* 28, 915-938.

Hutson, J.L. and Wagenet, R.J., 1995. A multiregion model describing water flow and solute transport in heterogeneous soils. *Soil Science Society of America Journal,* 59 (3), 743-751.

Jacques, D., Šimůnek, J., Mallants, D., et al., 2003. The HYDRUS-PHREEQC multicomponent transport model for variably-saturated porous media: code verification and application. *In:* Poeter, E., Zheng, C., Hill, M., et al. eds. *MODFLOW and more 2003: understanding through modeling: conference proceedings, International Ground Water Modeling Center, Colorado School of Mines, September 16-19, 2003.* Colorado School of Mines, Golden, 23-27.

Jarvis, N., 1998. Modeling the impact of preferential flow on nonpoint source pollution. *In:* Selim, H.M. and Ma, L. eds. *Physical nonequilibrium in soils: modeling and application.* Ann Arbor Press, Chelsea, 195-221.

Johnson, P.R. and Elimelech, M., 1995. Dynamics of colloid deposition in porous media: blocking based on random sequential adsorption. *Langmuir,* 11, 801-812.

Jury, W.A., Spencer, W.F. and Farmer, W.J., 1983. Behavior assessment model for trace organics in soil. I. Model description. *Journal of Environmental Quality,* 12 (4), 558-564.

Kan, A.T. and Tomson, M.B., 1990. Ground water transport of hydrophobic organic compounds in the presence of dissolved organic matter. *Environmental Toxicology and Chemistry,* 9 (3), 253-263.

Kretzschmar, R., Borkovec, M., Grolimund, D., et al., 1999. Mobile subsurface colloids and their role in contaminant transport. *Advances in Agronomy,* 66, 121-193.

Lawton, H.W. and Wilke, P.J., 1979. Ancient agricultural systems in dry regions. *In:* Hall, A.E., Cannell, G.H. and Lawton, H.W. eds. *Agriculture in semi-arid environments.* Springer, Berlin, 1-39.

Leij, F.J., Alves, W.J., Van Genuchten, M.T., et al., 1996. *The UNSODA Unsaturated Soil Hydraulic Database: user's manual version 1.0.* National Risk Management Laboratory, Cincinnati. Technical Report / Environmental Protection Agency no. EPA/600/R-96/095.

Leij, F.J., Šimůnek, J., Suarez, D.L., et al., 1999. Nonequilibrium and multicomponent transport models. *In:* Skaggs, R.W. and Van Schilfgaarde, J. eds. *Agricultural drainage.* American Society of Agronomy ASA, Madison, 405-430. Agronomy Monograph no. 38.

Lester, D.H., Jansen, G. and Burkholder, H.C., 1975. Migration of radionuclide chains through an adsorbing medium. *In:* Abrams, I.M., Zwiebel, I. and Sweed, N.H. eds. *Adsorption and ion exchange.* American Institute of Chemical Engineers, 202-213. AIChE Symposium Series no. 152, vol. 71.

Lichtner, P.C., 1996. Continuum formulation of multicomponent-multiphase reactive transport. *In:* Lichtner, P.C., Steefel, C.I. and Oelkers, E.H. eds. *Reactive transport in porous media.* Mineralogical Society of America, Washington, 1-81. Reviews in Mineralogy no. 34.

Lichtner, P.C., 2000. *FLOTRAN user manual.* Los Alamos National Laboratory, Los Alamos. Report LA-UR-01-2349.

Lichtner, P.C. and Seth, M.S., 1996. *User's manual for MULTIFLO. Part II.*

MULTIFLOW 1.0 and GEM 1.0: multicomponent-multiphase reactive transport model. Center for Nuclear Waste Regulatory Analyses, San Antonio. Report CNWRA no. 96-010.

Lindqvist, R. and Enfield, C.G., 1992. Biosorption of dichlorodiphenyltrichloroethane and hexachlorobenzene in groundwater and its implications for facilitated transport. *Applied and Environmental Microbiology,* 58 (7), 2211-2218.

Liu, C.W. and Narasimhan, T.N., 1989. Redox-controlled multiple-species reactive chemical transport. 1. Model development. *Water Resources Research,* 25 (5), 869-882.

Liu, H.H., Doughty, C. and Bodvarsson, G.S., 1998. An active fracture model for unsaturated flow and transport in fractured rocks. *Water Resources Research,* 34 (10), 2633-2646.

Liu, H.H., Zhang, G. and Bodvarsson, G.S., 2003. The active fracture model: its relation to fractal flow patterns and an evaluation using field observations. *Vadose Zone Journal,* 2 (2), 259-269. [http://vzj.scijournals.org/cgi/content/full/2/2/259]

Logan, B.E., Jewett, D.G., Arnold, R.G., et al., 1995. Clarification of clean-bed filtration models. *Journal of Environmental Engineering,* 121 (12), 869-873.

Magee, B.R., Lion, L.W. and Lemley, A.T., 1991. Transport of dissolved organic macromolecules and their effect on the transport of phenanthrene in porous media. *Environmental Science and Technology,* 25 (2), 323-331.

Mansfeldt, T., Leyer, H., Barmettler, K., et al., 2004. Cyanide leaching from soil developed from coking plant purifier waste as influenced by citrate. *Vadose Zone Journal,* 3 (2), 471-479. [http://vzj.scijournals.org/cgi/content/full/3/2/471]

Mattson, E.D., Ankeny, M.D., Šimůnek, J., et al., 2004. *Overland flow implications on surface cover designs, designing, building, & regulating evapotranspiration (ET) landfill covers, March 9-10, 2004, Denver, Colorado*. U.S. Environmental Protection Agency's Remediation Technology Development Forum (RTDF) Program, Grand Junction.

McCarthy, J.F. and McKay, L.D., 2004. Colloid transport in the subsurface: past, present and future challenges. *Vadose Zone Journal,* 3 (2), 326-337. [http://vzj.scijournals.org/cgi/content/full/3/2/326]

Misra, C., Nielsen, D.R. and Biggar, J.W., 1974. Soil nitrogen transformations during leaching. I. Theoretical considerations. *Soil Science Society of America Proceedings,* 38 (2), 289-293.

Mohanty, B.P., Bowman, R.S., Hendrickx, J.M.H., et al., 1998. Preferential transport of nitrate to a tile drain in an intermittent-flood-irrigated field: Model development and experimental evaluation. *Water Resources Research,* 34 (5), 1061-1076.

Mohanty, B.P., Bowman, R.S., Hendrickx, J.M.H., et al., 1997. New piecewise-continuous hydraulic functions for modeling preferential flow in an intermittent-flood-irrigated field. *Water Resources Research,* 33 (9), 2049-2063.

Morris, E.M. and Woolhiser, D.A., 1980. Unsteady one-dimensional flow over a plane: partial equilibrium and recession hydrographs. *Water Resources Research,* 16 (2), 355-360.

National Research Council, 2001. *Conceptual models of flow and transport in the fractured vadose zone*. National Academy Press, Washington.

Noell, A.L., Thompson, J.L., Corapcioglu, M.Y., et al., 1998. The role of silica colloids on facilitated cesium transport through glass bead columns and modeling. *Journal of Contaminant Hydrology,* 31 (1/2), 23-56.

Panday, S. and Huyakorn, P.S., 2004. A fully coupled physically-based spatially-

distributed model for evaluating surface/subsurface flow. *Advances in Water Resources,* 27 (4), 361-382.

Parkhurst, D.L. and Appelo, C.A.J., 1999. *User's guide to PHREEQC (version 2): a computer program for speciation, batch-reaction, one-dimensional transport, and inverse geochemical calculations.* U.S. Department of the Interior, U.S. Geological Survey, Denver. Water-Resources Investigations Report no. 99-4259.

Peters, R.R. and Klavetter, E.A., 1988. A continuum model for water movement in an unsaturated fractured rock mass. *Water Resources Research,* 24, 416-430.

Pinder, G.F. and Abriola, L.M., 1986. On the simulation of nonaqueous phase organic compounds in the subsurface. *Water Resources Research,* 22 (9 suppl.), 109-119.

Pruess, K., 1991. *TOUGH2: a general-purpose numerical simulator for multiphase fluid and heat flow.* Lawrence Berkeley Laboratory, Berkeley. Report no. LBL-29400.

Pruess, K. and Battistelli, A., 2002. *TMVOC: a numerical simulator for three-phase non-isothermal flows of multicomponent hydrocarbon mixtures in saturated-unsaturated heterogeneous media.* Lawrence Berkeley National Laboratory, Berkeley. Report LBNL no. 49375.

Pruess, K., Oldenburg, C. and Moridis, G., 1999. *TOUGH2 user's guide: version 2.0.* Lawrence Berkeley National Laboratory, Berkeley. Report LBNL no. 43134.

Rajagopalan, R. and Tien, C., 1976. Trajectory analysis of deep-bed filtration with the sphere-in-cell porous media model. *AIChE Journal,* 22, 523-533.

Rhoades, J.D., 1997. Sustainability of irrigation: an overview of salinity problems and control strategies. *In: Canadian Water Resources Association 50th annual conference: footprints of humanity: reflections on fifty years of water resource developments, Lethbridge, Alberta, Canada, June 3-6, 1997.* CWRA, 1-42.

Richards, L.A., 1931. Capillary conduction of liquids in porous media. *Physics,* 1, 318-333.

Ritsema, C.J., Dekker, L.W., Hendrickx, J.M.H., et al., 1993. Preferential flow mechanism in a water repellent sandy soil. *Water Resources Research,* 29 (7), 2183-2193.

Rittmann, B.E. and VanBriesen, J.M., 1996. Microbiological processes in reactive modeling. *In:* Lichtner, P.C., Steefel, C.I. and Oelkers, E.H. eds. *Reactive transport in porous media.* Mineralogical Society of America, Washington, 311-334. Reviews in Mineralogy no. 34.

Robbins, C.W., Wagenet, R.J. and Jurinak, J.J., 1980. A combined salt transport-chemical equilibrium model for calcareous and gypsiferous soils. *Soil Science Society of America Journal,* 44 (6), 1191-1194.

Rockhold, M.L., Yarwood, R.R. and Selker, J.S., 2004. Coupled microbial and transport processes in soils. *Vadose Zone Journal,* 3 (2), 368-383. [http://vzj.scijournals.org/cgi/content/full/3/2/368]

Rogers, V.C., 1978. Migration of radionuclide chains in groundwater. *Nuclear Technology,* 40 (3), 315-320.

Ross, P.J. and Smettem, K.R.J., 2000. A simple treatment of physical nonequilibrium water flow in soils. *Soil Science Society of America Journal,* 64 (6), 1926-1930.

Rubin, J., 1983. Transport of reacting solutes in porous media: relation between mathematical nature of problem formulation and chemical nature of reactions. *Water Resources Research,* 19 (5), 1231-1252.

Scanlon, B.R., Keese, K., Reedy, R.C., et al., 2003. Variations in flow and transport in thick desert vadose zones in response to paleoclimatic forcing (0-90 kyr): field

measurements, modeling, and uncertainties. *Water Resources Research,* 39 (7), 1179.

Schaap, M.G. and Leij, F.J., 2000. Improved prediction of unsaturated hydraulic conductivity with the Mualem-van Genuchten model. *Soil Science Society of America Journal,* 64 (3), 843-851.

Schaerlaekens, J., Mallants, D., Šimůnek, J., et al., 1999. Numerical simulation of transport and sequential biodegradation of chlorinated aliphatic hydrocarbons using CHAIN_2D. *Hydrological Processes,* 13 (17), 2847-2859.

Selim, H.M., Xue, S.K. and Iskandar, I.K., 1995. Transport of 2,4,6-trinitrotoluene and hexahydro-1,3,5-trintro-1,3,5-triazine in soils. *Soil Science,* 160 (5), 328-339.

Seuntjens, P., Mallants, D., Šimůnek, J., et al., 2002. Sensitivity analysis of physical and chemical properties affecting field-scale cadmium transport in a heterogeneous soil profile. *Journal of Hydrology,* 264 (1/4), 185-200.

Sheremata, T.W., Thiboutot, S., Ampleman, G., et al., 1999. Fate of 2,4,6-trinitrotoluene and its metabolites in natural and model soil systems. *Environmental Science and Technology,* 33 (22), 4002-4008.

Shikaze, S.G., Sudicky, E.A. and Mendoza, C.A., 1994. Simulation of dense vapor migration in discretely fractured geologic media. *Water Resources Research,* 30 (7), 1993-2009.

Šimůnek, J., Šejna, M. and Van Genuchten, M.T, 1999. *The HYDRUS-2D software package for simulating two-dimensional movement of water, heat, and multiple solutes in variably saturated media: version 2.0. IGWMC-TPS-53*. International Ground Water Modeling Center, Colorado School of Mines, Golden.

Šimůnek, J., Šejna, M. and Van Genuchten, M.T., 1998. *The HYDRUS-1D software package for simulating the one-dimensional movement of water, heat, and multiple solutes in variably-saturated media: version 2.0. IGWMC-TPS-70*. International Ground Water Modeling Center, Colorado School of Mines, Golden.

Šimůnek, J., Huang, K. and Van Genuchten, M.T., 1995. *The SWMS_3D code for simulating water flow and solute transport in three-dimensional variably saturated media: version 1.0*. USDA-ARS, U.S. Salinity Laboratory, Riverside, California. Research Report no. 139.

Šimůnek, J., Jarvis, N.J., Van Genuchten, M.T., et al., 2003. Review and comparison of models for describing non-equilibrium and preferential flow and transport in the vadose zone. *Journal of Hydrology,* 272 (1/4), 14-35.

Šimůnek, J. and Suarez, D.L., 1994. Two-dimensional transport model for variably saturated porous media with major ion chemistry. *Water Resources Research,* 30 (4), 1115-1133.

Šimůnek, J. and Suarez, D.L., 1997. Sodic soil reclamation using multicomponent transport modeling. *Journal of Irrigation and Drainage Engineering ASCE,* 123 (5), 367-376.

Šimůnek, J. and Valocchi, A.J., 2002. Geochemical transport. *In:* Dane, J.H. and Topp, G.C. eds. *Methods of soil analysis. Part 4. Physical methods*. SSSA, Madison, 1511-1536. SSSA Book Series no. 5.

Steefel, C.I., 2000. New directions in hydrogeochemical transport modeling: incorporating multiple kinetic and equilibrium reaction pathways. *In:* Bentley, L.R., Sykes, J.F., Brebbia, C.A., et al. eds. *Computational methods in water resources : proceedings 13th international conference*. Balkema, Rotterdam, 331-338.

Steefel, C.I. and MacQuarrie, K.T.B., 1996. Approaches to modeling of reactive transport in porous media. *In:* Lichtner, P.C., Steefel, C.I. and Oelkers, E.H. eds. *Reactive transport in porous media.* Mineralogical Society of America, Washington, 82-129. Reviews in Mineralogy no. 34.

Steefel, C.I. and Yabusaki, S.B., 1996. *OS3D/GIMRT: software for multicomponent-multidimensional reactive transport: user's manual and programmer's guide.* Pacific Northwest National Laboratory, Richland. Report PNNL no. 11166.

Stephens, D.B., Kowall, S.J., Borns, D., et al., 2002. Letter to the editor on A national strategy for vadose zone science and technology. *Vadose Zone Journal,* 1 (1), 197-198. [http://vzj.scijournals.org/cgi/content/full/1/1/197]

Strelkoff, T.S., Clemmens, A.J. and Schmidt, B.V., 1998. *SRFR version 3.31: a model for simulating surface irrigation in borders, basins and furrows.* U.S. Water Conservation Laboratory, USDA-ARS, Phoenix.

Tanji, K.K., 1990. *Agricultural salinity assessment and management.* ASCE, New York. ASCE Manuals and Reports on Engineering Practice no. 71.

Therrien, R. and Sudicky, E.A., 1996. Three-dimensional analysis of variably-saturated flow and solute transport in discretely-fractured porous media. *Journal of Contaminant Hydrology,* 23 (1/2), 1-44.

Thiele-Bruhn, S., 2003. Pharmaceutical antibiotic compounds in soils: a review. *Journal of Plant Nutrition and Soil Science,* 166 (2), 145-167.

Thompson, S.S. and Yates, M.V., 1999. Bacteriophage inactivation at the air-water-solid interface in dynamic batch systems. *Applied and Environmental Microbiology,* 65, 1186-1190.

Tolls, J., 2001. Sorption of veterinary pharmaceuticals in soils: a review. *Environmental Science and Technology,* 35 (17), 3397-3406.

Totsche, K.U. and Kögel-Knabner, I., 2004. Mobile organic sorbent affected contaminant transport in soil: numerical case studies for enhanced and reduced mobility. *Vadose Zone Journal,* 3 (2), 352-367. [http://vzj.scijournals.org/cgi/content/full/3/2/352]

U.S. Department of Energy, 2001. *A national roadmap for vadose zone science and technology: understanding, monitoring, and predicting contaminant fate and transport in the unsaturated zone. Revision 0.0.* U.S. Department of Energy. Report DOE no. ID-10871. [http://www.inel.gov/vadosezone/documents/roadmap.pdf]

Valocchi, A.J., Street, R.L. and Roberts, P.V., 1981. Transport of ion-exchanging solutes in groundwater: chromatographic theory and field simulation. *Water Resources Research,* 17 (5), 1517-1527.

Van Dam, J.C., Huygen, J., Wesseling, J.G., et al., 1997. *Theory of SWAP version 2.0: simulation of water flow, solute transport and plant growth in the Soil-Water-Atmosphere-Plant environment.* DLO Winand Staring Centre, Wageningen. Report / Wageningen Agricultural University, Department Water Resources no. 71.

Van Genuchten, M.T., 1985. Convective-dispersive transport of solutes involved in sequential first-order decay reactions. *Computers and Geosciences,* 11 (2), 129-147.

Van Genuchten, M.T. and Wagenet, R.J., 1989. Two-site/two-region models for pesticide transport and degradation: theoretical development and analytical solutions. *Soil Science Society of America Journal,* 53 (5), 1303-1310.

Van Genuchten, M.T. and Wierenga, P.J., 1976. Mass transfer studies in sorbing porous

media. I. Analytical Solutions. *Soil Science Society of America Journal,* 40 (4), 473-480.

VanBriesen, J.M., 1998. *Modeling coupled biogeochemical processes in mixed waste systems*. PhD Thesis Department of Civil Engineering, Northwestern University, Evanston.

VanderKwaak, J.E., 1999. *Numerical simulation of flow and chemical transport in integrated surface-subsurface hydrologic systems*. PhD Thesis Department of Earth Sciences, University of Waterloo, Ontario.

VanderKwaak, J.E. and Loague, K., 2001. Hydrologic-response simulations for the R-5 catchment with a comprehensive physics-based model. *Water Resources Research,* 37 (4), 999-1013.

Vinten, A.J.A., Yaron, B. and Nye, P.H., 1983. Vertical transport of pesticides into soil when adsorbed on suspended particles. *Journal of Agricultural and Food Chemistry,* 31 (3), 662-664.

Viswanathan, H.S., Robinson, B.A., Valocchi, A.J., et al., 1998. A reactive transport model of neptunium migration from the potential repository at Yucca Mountain. *Journal of Hydrology,* 209 (1/4), 251-280.

Von Gunten, H.R., Waber, U.E. and Krähenbühl, U., 1988. The reactor accident at Chernobyl: a possibility to test colloid-controlled transport of radionuclides in a shallow aquifer. *Journal of Contaminant Hydrology,* 2 (3), 237-247.

Wagenet, R.J. and Hutson, J.L., 1987. *LEACHM: leaching, estimation and chemistry model: a process-based model of water and solute movement, transformations, plant uptake and chemical reactions in the unsaturated zone*. Water Resources Institute, Cornell University, Ithaca.

Walter, A.L., Frind, E.O., Blowes, D.W., et al., 1994. Modeling of multicomponent reactive transport in groundwater. 2. Metal mobility in aquifers impacted by acidic mine tailings discharge. *Water Resources Research,* 30 (11), 3149-3158.

Wan, J. and Tokunaga, T.K., 2002. Partitioning of clay colloids at air-water interfaces. *Journal of Colloid and Interface Science,* 247 (1), 54-61.

Wang, Z., Jury, W.A., Tuli, A., et al., 2004. Unstable flow during redistribution: controlling factors and practical implications. *Vadose Zone Journal,* 3 (2), 549-559. [http://vzj.scijournals.org/cgi/content/full/3/2/549]

Wilson, G.V., Jardine, P.M. and Gwo, J.P., 1992. Modeling the hydraulic properties of a multiregion soil. *Soil Science Society of America Journal,* 56 (6), 1731-1737.

Woolhiser, D.A. and Liggett, J.A., 1967. Unsteady, one-dimensional flow over a plane: the rising hydrograph. *Water Resources Research,* 3 (3), 753-771.

Woolhiser, D.A., Smith, R.E. and Goodrich, D.C., 1990. *KINEROS: a kinematic runoff and erosion model: documentation and user manual*. U.S. Department of Agriculture, Agricultural Research Service. Report no. ARS-77.

Yeh, G.T., Salvage, K.M., Gwo, J.P., et al., 1998. *HYDROBIOGEOCHEM: a coupled model of hydrologic transport and mixed biochemical kinetic/equilibrium reactions in saturated-unsaturated media*. Oak Ridge National Laboratory, Oak Ridge. Report no. ORNL/TM-13668.

Yeh, G.T. and Tripathi, V.S., 1990. *HYDROGEOCHEM: a coupled model of hydrological and geochemical equilibrium of multicomponent systems*. Oak Ridge National Laboratory, Oak Ridge. Report no. ORNL-6371.

Zhang, P.F., Šimůnek, J. and Bowman, R.S., 2004. Nonideal transport of solute and colloidal tracers through reactive zeolite/iron pellets. *Water Resources Research,* 40 (4), NIL_1-NIL_11.

Zhang, W. and Cundy, T.W., 1989. Modeling of two-dimensional overland flow. *Water Resources Research,* 25 (9), 2019-2035.

Zurmühl, T. and Durner, W., 1996. Modeling transient water and solute transport in a biporous soil. *Water Resources Research,* 32 (4), 819-829.

Zyvoloski, G.A., Robinson, B.A., Dash, Z.V., et al., 1997. *Summary of the models and methods for the FEHM application: a finite element heat- and mass-transfer code*. Los Alamos National Laboratory, Los Alamos. Report no. LA-13307-MS.